

2

AD-A208 764

# NAVAL POSTGRADUATE SCHOOL

## Monterey, California



# THESIS

Thermomechanical Processing of Aluminum Alloy  
2090 For Superplasticity

by

Mohammad B. Choudhry

March 1989

Thesis Advisor:

Terry R. McNelley

Approved for public release; distribution is unlimited

~~SECRET~~  
SDTIC  
ELECTE  
JUN 09 1989  
H

89' 6 03 027

UNCLASSIFIED

SECURITY CLASSIFICATION OF THIS PAGE

## REPORT DOCUMENTATION PAGE

1a REPORT SECURITY CLASSIFICATION UNCLASSIFIED			1b RESTRICTIVE MARKINGS	
2a SECURITY CLASSIFICATION AUTHORITY			3 DISTRIBUTION AVAILABILITY OF REPORT Approved for public release; distribution is unlimited	
2b DECLASSIFICATION/DOWNGRADING SCHEDULE				
4 PERFORMING ORGANIZATION REPORT NUMBER(S)			5 MONITORING ORGANIZATION REPORT NUMBER(S)	
6a NAME OF PERFORMING ORGANIZATION Naval Postgraduate School	6b OFFICE SYMBOL (If applicable) 69	7a NAME OF MONITORING ORGANIZATION Naval Postgraduate School		
6c ADDRESS (City, State, and ZIP Code) Monterey, CA 93943-5000		7b ADDRESS (City, State, and ZIP Code) Monterey, CA 93943-5000		
8a NAME OF FUNDING SPONSORING ORGANIZATION	8b OFFICE SYMBOL (If applicable)	9 PROCUREMENT INSTRUMENT IDENTIFICATION NUMBER		
8c ADDRESS (City, State, and ZIP Code)		10 SOURCE OF FUNDING NUMBERS		
		PROGRAM ELEMENT NO	PROJECT NO	TASK NO
		WORK UNIT ACCESSION NO		
11 TITLE (Include Security Classification) Thermomechanical Processing of Aluminum Alloy 2090 for Superplasticity				
12 PERSONAL AUTHOR(S) Mohammad B. Choudhry				
13a TYPE OF REPORT Master's Thesis	13b TIME COVERED FROM _____ TO _____	14 DATE OF REPORT (Year, Month, Day) 1989, March	15 PAGE COUNT 85	
16 SUPPLEMENTARY NOTES: "The views expressed in this thesis are those of the author and do not reflect the official policy or position of the Department of Defense or the U.S. Government."				
17 COSAT CODES			18 SUBJECT TERMS (Continue on reverse if necessary and identify by block number)	
FIELD	GROUP	SUB-GROUP	Thermomechanical, Superplasticity, TMP	
			Micrograph, Recrystallization	
19 ABSTRACT (Continue on reverse if necessary and identify by block number) <i>ABSTRACT</i> The effect of processing variables on the microstructural development and superplasticity of aluminum alloy 2090, a high strength Al-Cu-Li-Zr alloy of reduced density in comparison to other Al-based materials, was investigated. Following previous research, warm rolling was conducted to strains up to 3.36 and it was found that increasing the strain to values greater than 2.6 offered no improvement in subsequent superplastic response. Increased rolling speeds likewise did not enhance ductibility above a maximum value of approximately 240 percent. Microstructural examination revealed a refined, homogeneous microstructure consisting of T <sub>2</sub> particles distributed in an alloy matrix. These particles reside a triple junctions in a recovered microstructure.				
20 DISTRIBUTION AVAILABILITY OF ABSTRACT <input checked="" type="checkbox"/> UNCLASSIFIED UNLIMITED <input type="checkbox"/> SAME AS RPT <input type="checkbox"/> DTIC USERS			21 ABSTRACT SECURITY CLASSIFICATION UNCLASSIFIED	
22a NAME OF RESPONSIBLE INDIVIDUAL Professor Terry R. McNelley			22b TELEPHONE (Include Area Code) (408) 646-2589	22c OFFICE SYMBOL 69Mc

Approved for public release; distribution is unlimited.

Thermomechanical Processing of Aluminum Alloy  
2090 for Superplasticity

by

Mohammad B. Choudhry  
Lieutenant Commander, Pakistan Navy  
B. E. (Mech), NED University Karachi Pakistan

MASTER OF SCIENCE IN MECHANICAL ENGINEERING

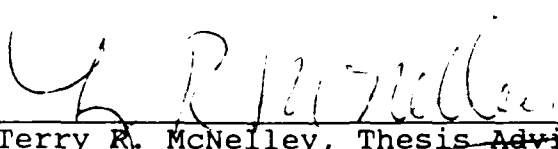
from the


NAVAL POSTGRADUATE SCHOOL  
March 1989

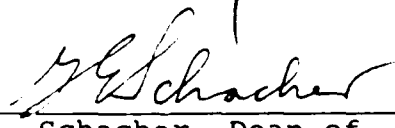
Author:

  
Mohammad B. Choudhry

Approved:

  
Terry R. McNeley, Thesis Advisor

  
Anthony J. Healey, Chairman,  
Department of Mechanical Engineering

  
Gordon E. Schacher, Dean of  
Science and Engineering

### ABSTRACT

The effect of processing variables on the micro-structural development and superplasticity of aluminum alloy 2090, a high strength Al-Cu-Li-Zr alloy of reduced density in comparison to other Al-based materials, was investigated. Following previous research, warm rolling was conducted to strains, up to 3.36 and it was found that increasing the strain to values greater than 2.6 offered no improvement in subsequent superplastic response. Increased rolling speeds likewise did not enhance ductibility above a maximum value of approximately 240 percent. Microstructural examination revealed a refined, homogeneous microstructure consisting of  $T_2$  particles distributed in an alloy matrix. These particles reside at triple junctions in a recovered microstructure.



Accession For	
NTIS GFA&I	<input checked="checked" type="checkbox"/>
DTIC TAB	<input type="checkbox"/>
Unannounced	<input type="checkbox"/>
Justification	
By	
Distribution/	
Availability Codes	
Dist	Avail and/or Special
A-1	

## TABLE OF CONTENTS

	PAGE
I. INTRODUCTION-----	1
II. BACKGROUND-----	5
A. HISTORY OF DEVELOPMENT OF ALUMINUM-----	5
B. SUPERPLASTICITY AND SUPERPLASTIC FORMING----	7
1. PROCESS-----	7
2. STRAIN RATE SENSITIVITY COEFFICIENT----	9
C. OBJECTIVE OF THIS RESEARCH-----	11
III. EXPERIMENTAL PROCEDURE-----	13
A. MATERIAL-----	13
B. PROCESSING-----	13
1. SOLUTION TREATMENT AND FORGOING-----	13
2. WARM ROLLING-----	16
C. TENSILE TESTING-----	18
D. METALLOGRAPHY-----	21
IV. RESULTS AND DISCUSSION-----	23
A. MICROSTRUCTURE CONDITION-----	23
PRIOR TO ROLLING	
B. MICROSTRUCTURAL CONDITION-----	25
AFTER ROLLING	
C. MECHANICAL PROPERTIES-----	30
D. EFFECT OF DEFORMATION ON MICROSTRUCTURE----	43
E. SUMMARY-----	50
V. CONCLUSIONS-----	52

VI. RECOMMENDATIONS-----	53
APPENDIX A - SUMMARY OF DUCTILITY DATA-----	54
APPENDIX B - TENSILE TEST DATA-----	55
LIST OF REFERENCES-----	70
INITIAL DISTRIBUTION LIST-----	73

## LIST OF FIGURES

	PAGE
Figure 1. Schematic Representation of the Thermomechanical Processing for the Material Rolled to 2.60 True Strain.	-----14
Figure 2. Schematic Representation of the Thermomechanical Processing for the Material Rolled to 3.36 True Strain.	-----15
Figure 3. Plate to Test Specimen Geometry.	-----19
Figure 4. Tensile Test Sample Configuration and Dimensions. The Effective Gage Length is 0.50 Inches and the Thickness is Function of Final Rolling Strain. The Specimen was Machined in Parallel to the Rolling Direction.	-----20
Figure 5. Long Transverse Optical Micrograph of Alloy 2090 Following Solution Treatment at 540°C for 8 Hours, Forged to 25.4mm at 480°C, Annealed for 4 Hours at 540°C and Quenched in Cold Water.	-----24
Figure 6. Rolled Surface Section (a) and Long Transverse Section (b) Optical Micrographs of Alloy 2090 Following Rolling at 300°C to a True Strain of 3.36 with 30 Minutes Reheating Intervals Between Passes.	-----26
Figure 7. Rolled Surface Section (a) and Long Transverse Section (b) Optical Micrographs of Alloy 2090 Following Rolling at 300°C to a True Strain of 2.60 with 30 Minutes Reheating Intervals Between Passes at Higher Rolling Speed.	-----27
Figure 8. Rolled Surface Section (a) and Long Transverse Section (b) Optical Micrographs of Alloy 2090 Following Rolling at 300°C to a True Strain of 2.60 with 30 Minutes Reheating Intervals Between Passes at Lower Rolling Speed.	-----28

- Figure 9. Long Tranverse Section Optical Micro-----29  
graph of Alloy 2090 Specimen Following  
Rolling at 300 °C to a True Strain of  
3.36 with 30 Minutes Reheating  
Intervals Between Passes and Annealing  
at 540 °C for 10 Minutes.
- Figure 10. Ductility vs. Tensile Test Temperature-----32  
for Various TMP Schedules Shown in the  
Legend. The Material was Rolled in the  
Original Plate Longitudinal Direction  
with True Strain of 3.36.
- Figure 11. Flow Stress at Strain of 0.1 -----33  
The Material was Rolled in the Original  
Longitudinal Plate Direction to a  
Rolling Strain of 3.36.
- Figure 12. Ductility vs. Tensile Test Temperature-----34  
for Various TMP Schedules Shown in the  
Legend. The Material was Rolled in the  
Original Plate Longitudinal Direction  
with True Strain of 2.60 at High Rolling  
Speed.
- Figure 13. Flow Stress at Strain of 0.1 -----35  
The Material was Rolled in the Original  
Longitudinal Plate Direction to a  
Rolling Strain of 2.60 at Higher Rolling  
Speed.
- Figure 14. Ductility vs. Tensile Test Temperature-----36  
for Various TMP Schedules Shown in the  
Legend. The Material was Rolled in the  
Original Plate Longitudinal Direction  
with True Strain of 2.60 at Lower Rolling  
Speed.
- Figure 15. Flow Stress at Strain of 0.1-----37  
The Material was Rolled in the  
Original Longitudinal Plate Direction  
to a Rolling Strain of 2.60 at Lower  
Rolling Speed
- Figure 16. Flow Stress vs. Strain Rate at Strain-----39  
of 0.1 for Material Rolled to 3.36 True Strain.



- Figure 17. Ductility vs. Temperature for Various-----41  
TMP Schedules Shown in the Legend.  
The Material was Rolled to a True  
Strain of 3.36 in the Original  
Longitudinal Plate Direction.
- Figure 18. Comparison of Flow Stress at a Strain-----42  
Rate of  $6.67 \times 10^{-4} \text{ s}^{-1}$ . The Material  
was Rolled to a True Strain of 3.36.
- Figure 19. Long Tranverse Gage Section (a) and-----44  
Grip Section (b) Optical Micrographs  
of Alloy 2090 Following Tensile Test  
Conducted at  $400^\circ \text{C}$  at Strain Rate of  
 $6.67 \times 10^{-4} \text{ s}^{-1}$ . The Material was  
Rolled at  $300^\circ \text{C}$  To a True Strain of 3.36  
with 30 Minutes Reheating Intervals  
Between Passes. The Microstructure is  
Similiar to as Rolled Conditions and  
Coarsening has not Taken Place.
- Figure 20. Long Tranverse Gage Section (a) and-----46  
Grip Section (b) Optical Micrographs  
of Alloy 2090 Following Tensile Test  
Conducted at  $400^\circ \text{C}$  at Strain Rate of  
 $6.67 \times 10^{-4} \text{ s}^{-1}$ . The Material was  
Rolled at  $300^\circ \text{C}$ . To a True Strain of  
3.36 with 30 Minutes Reheating Intervals  
Between Passes. The Cavitation Along  
the Boundaries is very Clear at  $500^\circ \text{C}$ .
- Figure 21. Long Tranverse Gage Section (a) and-----47  
Grip Section (b) Optical Micrographs  
of Alloy 2090 Following Tensile Test  
Conducted at  $400^\circ \text{C}$  at Strain Rate of  
 $6.67 \times 10^{-4} \text{ s}^{-1}$ . The Material was  
Rolled at  $300^\circ \text{C}$ . To a True Strain of  
3.36 with 30 Minutes Reheating Intervals  
Between Passes. The Specimen was Annealed  
at  $540^\circ \text{C}$  for 10 Minutes before Conducting  
Tensile Tests.

Figure 22. Long Tranverse Gage Section (a) and-----49  
Grip Section (b) Optical Micrographs  
of Alloy 2090 Following Tensile Test  
Conducted at 500°C at Strain Rate of  
 $6.67 \times 10^{-4} \text{ S}^{-1}$ . The Material was  
Rolled at 300°C. To a True Strain of  
3.36 with 30 Minutes Reheating Intervals  
Between Passes. The Specimen was Annealed  
at 540°C for 10 Minutes before Conducting  
Tensile Tests. Concentration of  
Cavitation on Grain Boundaries is Clearly  
Evident in Gage Section, Particularly  
Towards the Necking.

## ACKNOWLEDGEMENT

I would like to thank my advisor, Professor T. R. McNelley for the skilled guidance and tireless assistance provided during this research. The technical assistance provided by Mr. T. Kellogg and Mr. R. Hafley of the Naval Postgraduate School and Mr. James Wu of Lawrence Labs Berkley is also appreciated. I would also like to express my sincere appreciation to my wife, Rahila and our three children, Ayesha, Shiraz, and Shehzad for their dedicated support of my work at the Naval Postgraduate School.

## I. INTRODUCTION

In recent years significant advances have been made in new manufacturing techniques by utilizing improved capabilities of some new materials. Superplasticity is one notable quality of some materials, which facilitates fabrication of complex part geometries in a single forming operation. Superplastic forming is an emerging technology which has the potential of offering improved performance through reduced weight, increased reliability, reduced number of parts, and cost savings in certain structural applications.

The ability of some materials to sustain large tensile elongations without localized necking is known as superplasticity. Generally, materials which exhibit elongations of 200 percent or greater are considered to be superplastic. However, certain materials are capable of experiencing 2000-3000 percent elongations under specific temperature and controlled strain rate [Ref. 1].

Superplastic forming is based on superplastic ductilities, attainable in certain materials through controlled processing. The materials with superplastic forming capability, particularly aluminum-based alloys, have attracted the attention of the aerospace industry

over the past few years [Ref. 2]. The automotive industry may also be able to utilize such materials, although the presently available slow forming rates preclude use in this field. Thus, the aerospace industries have played the most significant role in applying new materials for manufacturing of structural components. By eliminating fasteners, superplastic forming improves fatigue and corrosion performance, and the availability of such materials is vital for aerospace structural applications.

Aluminum based alloys have been in general use in aerospace applications since the 1930's. Over time, the aluminum-lithium alloys have become of interest due to their reduced density and increased modulus of elasticity relative to pure aluminum. The aluminum alloy 2090 (Al-2.56 Wt% Cu-2.03 Wt% Li-0.12 Wt% Zr) was developed by Alcoa and is seven to eight percent less dense and has Young's modulus ten percent higher than that of 7075 aluminum alloy [Ref. 3].

Beryllium is another element which, when utilized as an alloying element with aluminum, provides similar results as lithium. However, it is not widely used because of certain severe draw backs, specifically the need of sophisticated manufacturing techniques such as powder metallurgy, and also the toxicity of BeO, the oxide of beryllium [Ref. 4].

Although Al-Li alloys exhibit poor fatigue and fracture resistance, this can be overcome by addition of Cu. The concept of adding copper to improve fatigue and fracture characteristics was applied by Alcoa in developing and registering the 2090 composition in the early 80's.

This present research was undertaken to investigate the superplastic behavior of Al-2090 alloy in conjunction with a thermomechanical process (TMP) developed at the Naval Postgraduate School (NPS). Basically, this TMP was devised to investigate superplastic response of Al-Mg alloys and later was extended to Al-Mg-Li alloys. The purpose of using this TMP was to promote microstructural changes via the continuous recrystallization (CRX) mechanism in a manner similar to that utilized with Al-Mg and Al-Mg-Li-Zr alloys previously studied at NPS [Ref. 5]. The process involves solution treatment, i.e. initial homogenization, hot working and then warm rolling to a comparatively large accumulated rolling strain. In this process, warm rolling creates high density of dislocations, which in turn promotes CRX through static recovery while reheating between the rolling passes. The process also utilizes the precipitation of intermetallic phases such as  $T_2$ , in 2090 or  $(Al_8Mg_5)$  in Al-Mg-X alloys [Ref. 5].

Previous work conducted at NPS on Al-2090 has attempted to adapt the work on Al-Mg alloys to Al-2090. Spiropoulos [Ref. 3] worked on attaining uniform distribution of  $T_1$  precipitates by combination of cold work and aging treatments, assuming that the  $T_1$  would facilitate CRX during warm rolling. The results obtained were not encouraging and the process failed to create recrystallized conditions. Regis [Ref. 6] and Groh [Ref. 7] continued their work to obtain CRX through the same TMP with some minor changes. Groh utilized a true rolling strain of 2.50 and obtained a microstructure consisting predominately of  $T_2$  precipitates at the conclusion of warm rolling. The details of the precipitation sequence are explained in Ref. 7. It was suggested by Groh that higher accumulated rolling strain may result in a finer microstructure, and CRX via static recovery, during processing. To investigate this, the rolling strain was increased beyond 2.50 in this study. The effect of higher rolling speed was also studied and comparison made by rolling the material at two different rolling speeds. To improve the initial homogenization of structure, the period of solution treatment was also increased and the cold work previously incorporated was deleted from the TMP.

## II. BACKGROUND

### A. HISTORY OF DEVELOPMENT OF ALUMINUM ALLOY 2090

The development of new materials for aerospace use started during the World War I, when the manufacturing of aircraft structures began shifting from wood and fabric to metal frames. By 1930, with the standardization of stressed wing skin design, the use of metals, particularly aluminum, had become firmly established in this industry [Ref. 8]. The need for weight saving and increasing load carrying capabilities brought about the use of other elements in alloying with aluminum. Although Al-Li alloys have been developed intermittently since the 1920's, it was in 1957 when such material, designated as Al-2020, was first used in aircraft applications [Ref. 8]. As every one weight percent addition of lithium reduces the density of aluminum by three percent and increases the alloy modulus of elasticity by six percent, the Al-Li alloys showed a great potential for structural applications [Ref. 9]. In critical applications, precise control of surface appearance, the absence of internal defects, uniform cast grain size and low impurity contents are important requirements of any material and are readily controlled



in Al-Li alloys [Ref. 10]. However, fracture toughness of Al-Li alloys is known to be poor and while Al-2020 performed satisfactorily in service, it would not meet current requirements for fracture toughness at strengths attainable via heat treatment, resulting in limiting the use of Al-Li alloys in aerospace applications.

The emergence of composites in the 70's momentarily diverted the attention of the research community away from aluminum alloys [Ref. 9]. Although composites offered very favorable qualities, they also required large expenditure on new, compatible aircraft manufacturing facilities. In recognition of the competition from composites, the aluminum-lithium alloys again became the focal point of research. In 1981, Alcoa launched "Alithalite", a project to develop low density replacements for several commercial alloys. To improve fracture toughness and resistance to stress corrosion cracking, copper and zirconium were added to Al-Li alloys. A low percentage of zirconium in Al-Li alloy increases the recrystallization temperature and also results in enhancing the superplastic properties by acting as grain refiner [Ref. 3]. Thus Alcoa developed

an alloy containing Al-2.7 Wt% Cu-2.2 Wt% Li-0.12 Wt% Zr, which was registered as Al-2090 in 1984 [Ref. 9]. The improved fatigue resistance, increased elastic modulus and reduced density combine to make Al-2090 a strong candidate material for many aerospace applications.

## B. SUPERPLASTICITY AND SUPERPLASTIC FORMING

### 1. Process

The phenomenon of extended elongation without localized necking is known as superplasticity. Research work in this area was initially undertaken by Soviet scientists [Ref. 11]. Although they did not use the term "superplasticity", their work documented considerable elongations in a number of materials. Underwood [Ref. 11], wrote the first English language review of superplasticity in 1962 and generated the interest of the western world in this field [Ref. 12].

In the earliest work on superplasticity, this phenomenon was recognized as an elevated temperature process. In 1946, Kayushnikov related increased plasticity in steels to phase changes above 700 °C. Gueussier and Castro [Ref 11] determined the hot ductilities of ferrous metals in torsion and attributed this to continuous recrystallization during deformation.

It was also established by 1970 that a fine grain structure is one of the controlling factors in achieving

appreciable superplasticity [Ref. 2]. Further research suggested that uniform distribution of second phase precipitates and mobile high angle grain boundaries are essential, along with fine grain size, for promoting superplastic ductility [Ref. 13, 14]. A uniformly distributed second phase is necessary to retard grain growth at elevated temperatures and the high angle boundaries facilitate the sliding of grain boundaries and enhance the superplastic properties [Ref. 13].

As mentioned earlier, Underwood's review of superplasticity in 1962 acted as catalyst for starting extensive research work in this field. A number of methods were proposed to achieve the above mentioned microstructure. With respect to aluminum, the most commonly adopted methods are that proposed by researchers at Rockwell [Ref. 15, 16] and that developed at Alcan for Supral (Al-Cu-Zr) alloys. The details of the Rockwell thermomechanical processing are given in Ref. 16. In the case of the Supral alloys, continuous recrystallization is utilized to obtain fine microstructure with high angle grain boundaries [Ref. 17]. The continuous recrystallization, during heating after deformation processing, initially results in subgrain structure by

rearrangement of dislocations produced by straining during rolling. This structure then evolves into a fine grain microstructure with relatively high angle boundaries facilitating subsequent superplastic straining [Ref. 17, 18].

A thermomechanical process has been developed at the Naval Postgraduate School for acquiring requisite micro structural characteristics for superplastic forming. This method is based on introduction of dislocations by rolling at a sufficient temperature that recovery followed by continuous recrystallization occurs while annealing between the rolling passes, resulting in a refined grain structure after enough cycles of deformation and annealing [Ref. 19, 20]. The method has been successfully used at NPS to promote superplasticity in Al-Mg-X alloys at moderate temperatures. This technique has been extended to Al-Mg-Li-X alloys by a number of researchers at NPS as well as to 2090 alloy.

## 2. Strain Rate Sensitivity Coefficient

The flow stress depends upon strain rate, temperature and the microstructure of the material. The relation between flow stress  $\sigma_f$  and strain rate  $\dot{\epsilon}$  at constant strain and temperature is

$$\sigma_f = C \dot{\epsilon}^m | \epsilon, T$$

where C is a material constant and m is known as strain rate sensitivity coefficient [Ref. 21]. The value of m is calculated from the experimental data through the equation:

$$m = \frac{d(\ln \dot{\epsilon})}{d(\ln \sigma)}$$

The value of m is highly influenced by strain rate, temperature and the microstructure of the material. Typical values of m for superplastic material range from 0.3 to 0.9. Higher values of m help in avoiding premature fracture during elongation and hence are a direct measure of resistance to local plastic instability in a material. However, material even having  $m > 0.3$  sometimes may fracture prematurely due to tensile failure of grain boundaries due, for example, to impurities in the material [Ref. 1].

Along with temperature above about  $0.5T_m$  and low strain rate, a fine microstructure is essential to large values of this coefficient. At low temperatures, the grain boundaries of fine grains act as barriers to dislocation motion whereas at elevated temperatures, the large area of the grain boundaries helps in superplastic flow by facilitating mass transport of atoms along the boundaries or by providing

a short distance across the grains [Ref. 22]. Another notable fact is that the required refined grain structure can only be achieved in many alloys by introduction of fine particles of a dispersoid, such as  $\text{Al}_3\text{Zr}$  in Al-2090. The presence of such fine particles creates resistance to coarsening of grains at higher temperatures, maintaining a stable value of  $m$  over a range of temperature.

#### C. OBJECTIVE OF THIS RESEARCH

A fine grain size with high angle grain boundaries is generally considered to facilitate superplasticity [Ref. 23]. To obtain this type of microstructure through continuous recrystallization (CRX), the thermomechanical process (TMP) developed at NPS has successfully been employed on Al-Mg alloys. The requirements have been attained in work on Al-Mg alloys by a thermomechanical process concluding with isothermal rolling at temperature near  $300^\circ\text{C}$ . Such a temperature is below the solvus for Mg and thus precipitation of the intermetallic  $\epsilon$  phase occurs concurrently with intervals of straining and recovery. Continuous recrystallization may be facilitated during such processing by controlling the strain per pass, the reheating interval and the total strain such that the precipitating intermetallic  $\epsilon$  phase stabilizes recovering dislocation arrays. If dislocations can continue to recover to such

sub-boundaries, the boundaries may be caused to increase progressively in misorientations and convert to boundaries capable of sustaining superplastic deformation mechanisms.

Studies regarding application of this concept to Al-2090 began with Spiropoulos [Ref. 3] and most recently concluded with Groh [Ref. 7]. The previous work has demonstrated that  $T_2$  phase may play the same role as  $\delta$  phase in Al-Mg alloys. The microstructure obtained at the end of processing by Groh consisted of fine subgrains stabilized by  $T_2$ , i.e., insufficient boundary misorientation was achieved [Ref 7].

One conclusion of Groh's work was that increased rolling strain in conjunction with controlled reheating may facilitate formation of more highly misorientated boundaries and thus enhance superplasticity beyond the 300% elongation attained. The objective of this research work is to investigate this hypothesis by incorporating higher total rolling strain during the TMP.

### III. EXPERIMENTAL PROCEDURE

#### A. MATERIAL

The composition of aluminum alloy (Al-2090) studied in this research is given in Table 1. The material was provided in the form of rolled plate 51cm long, 31cm wide and 4.2cm thick heat treated to a T8A41 tempered condition.

TABLE I.

COMPOSITION OF AL-2090 (WT. PCT.)

	Cu	Li	Zr	Al
Al-2090	2.4-3.0	1.9-2.6	0.08	Bal
This alloy	2.56	2.03	0.12	Bal

#### B. PROCESSING

The thermomechanical processing (TMP) schemes employed in this study are illustrated in Figures 1 and 2. The details of the processing are given below.

##### 1. Solution Treatment and Forging

The solution treatment process was intended to produce a uniform solid solution by dissolving the soluble components in the alloy. To accomplish this,



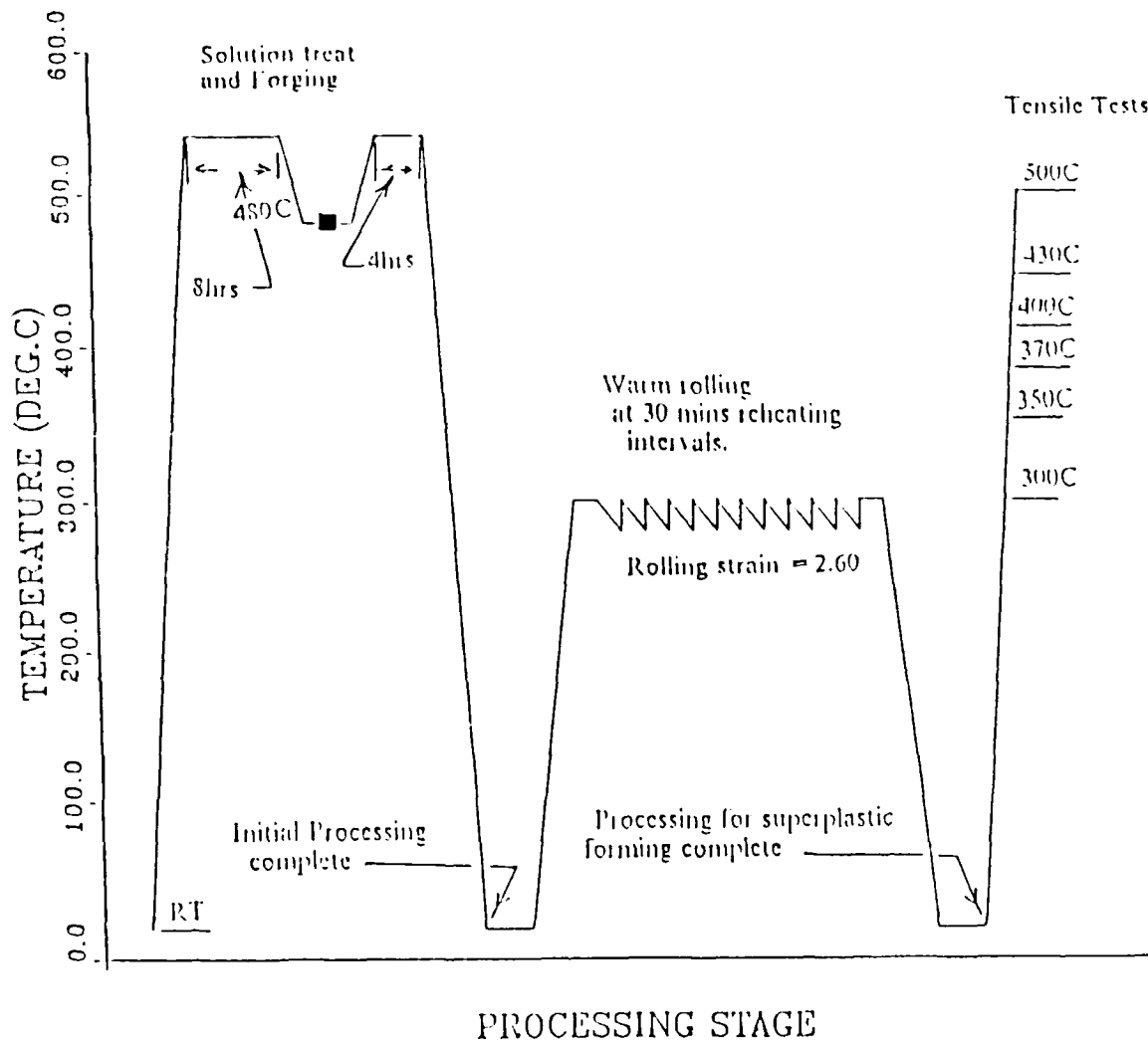


Figure 1. Schematic Representation Of The Thermomechanical Processing For The Material Rolled To 2.60 True Strain.

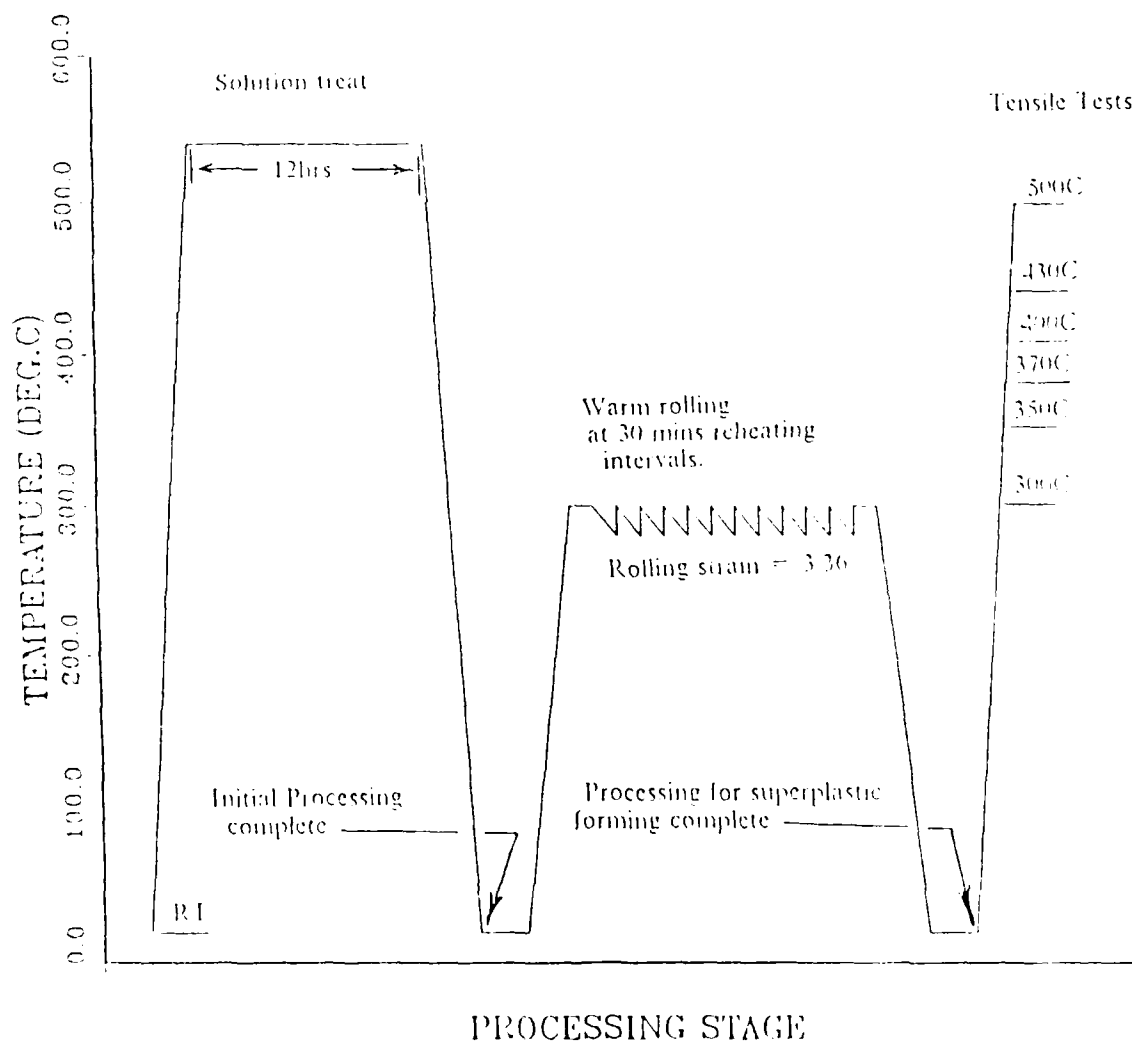


Figure 2. Schematic Representation Of The Thermo-mechanical Processing For The Material rolled to 3.36 True Strain.

blocks 42mm x 43mm x 51mm previously sectioned from the material were held at 540°C for 12 hours, well above the solvi for T<sub>1</sub> and T<sub>2</sub> phases. Two blocks were forged in the short transverse direction to 25.4mm thickness, after eight hours at 540°C, and were again heated for four hours at 540°C. The forging was carried out in a Baldwin-Tate-Emery Universal testing machine between two platens heated to 480°C (maximum allowable temperature of the platen material). The third billet was held at 540°C for 12 hours and was not forged. In all three cases, the billets were cold-water quenched at the end of the total 12 hours solution treating. One of the forged billets was sectioned into two pieces to facilitate rolling at the Naval Postgraduate School, whereas the other two were left as single pieces.

## 2. Warm Rolling

This critical step in the TMP is performed under a combination of parameters to convert the microstructure to one capable of supporting superplasticity. To promote CRX, a sequence of rolling and annealing treatments are conducted, so that the recovery of dislocations, produced during rolling, will ultimately form refined grains with high-angle boundaries.

TABLE II.

## ROLLING SCHEDULE

ROLL DIA = 305 mm				ROLL DIA = 113 mm	
BILLET - 1		BILLET - 2		BILLET - 3	
Rolling Pass	Thickness (mm)	Rolling Pass	Thickness (mm)	Rolling Pass	Thickness (mm)
0	42.0				
1	36.8			0	25.4
2	31.8			1	22.9
3	26.7	0	25.4	2	20.3
4	21.6	1	21.6	3	17.8
5	16.5	2	16.5	4	15.2
6	11.4	3	11.4	5	12.7
7	8.3	4	8.3	6	9.5
8	5.1	5	5.1	7	6.2
9	4.1	6	4.1	8	4.3
10	3.0	7	3.0	9	2.5
11	1.9	8	1.92	10	1.98
12	1.45				

Warm rolling was conducted at a temperature of 300 °C utilizing two different rolling speeds. The details of rolling schemes and the schedule of rolling reductions are summarized in Table II. The material was preheated to the rolling temperature of 300 °C for 30 minutes and subsequently 30 minute reheating intervals were utilized between rolling passes. A true strain of 3.36 in unforged and 2.60 in forged material was obtained at the end of warm rolling. It is to be noted that a true strain of 2.60 was obtained in two cases at two different rolling speeds as indicated in Table II. In all cases the reduction per rolling pass was reduced in final passes to avoid cracking of the material. A steel plate 1" X 6" X 12" in size was used to facilitate isothermal conditions. At the end of rolling, the rolled sample thicknesses of 1.92mm and 1.47mm, corresponding to true strain of 2.60 and 3.36, respectively, were achieved. Figure 3 provides a schematic illustration of the three processing conditions.

#### C. TENSILE TESTING

Upon completion of warm rolling, the material was machined into tensile test samples in accordance with the design shown in Figure 4. The samples were prepared keeping the tensile test axis parallel to the prior TMP

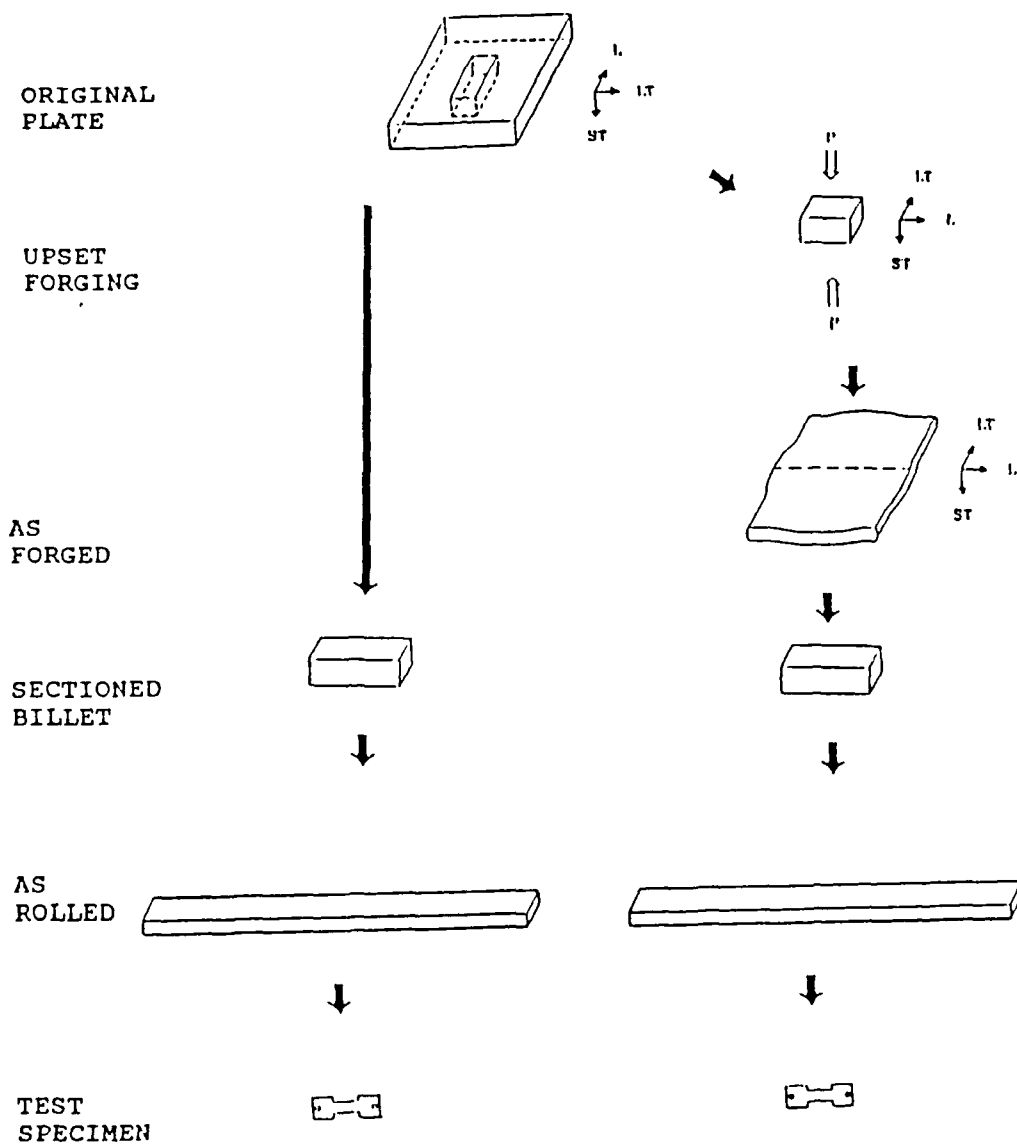
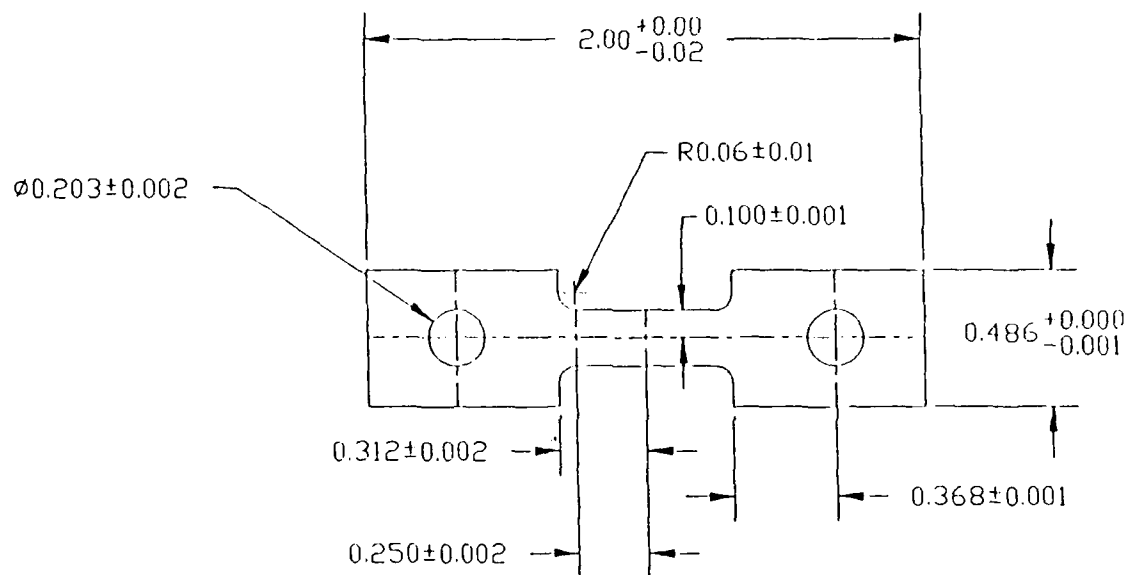


Figure 3. Plate To Test Specimen Geometry

# TENSILE SAMPLE GEOMETRY



Note: All dimensions are in inches.

Figure 4. Tensile Test Sample Configuration And Dimensions. The Effective Gage Length Is 0.50 Inches And The Thickness Is Function Of Final Rolling Strain. The Specimen Was Machined in Parallel To The Rolling Direction.

rolling direction. A set of the samples previously rolled to a strain of 3.36 was annealed at 540°C for ten minutes to provide a comparison to the tensile test results with as-rolled material.

Tensile testing on material from each of the TMP process variants were performed at 300 °C , 350 °C , 370 °C, 400 °C, 430 °C, and 500 °C at crosshead speeds corresponding to an engineering strain rate ranging from  $6.67 \times 10^{-5} \text{ s}^{-1}$  to  $6.67 \times 10^{-2} \text{ s}^{-1}$  on an Instron model 1102 testing machine, utilizing a Marshal single-zone furnace to heat the specimens to test temperature. The specimens were held in the furnace for approximately 40 minutes prior to the beginning of each tensile test to allow for the temperature to equilibrate. In addition to the furnace controller, the test temperature was monitored by two thermocouples placed along the length of the test specimen. Load versus time data were autographically recorded and converted to true stress versus true strain, compensating for decrease in true strain rate with increasing strain.

#### D. METALLOGRAPHY

The optical microscopy was conducted on the material prior to and after warm rolling and on selected specimens after the tensile testing. The samples annealed at 540°C for ten minutes and tested at various temperatures were



also observed through optical microscopy. The samples were cold mounted and mechanically polished by using 6, 3, and 1 micron diamond paste in succession. Final polishing was done using cerium oxide paste, diluted with distilled water. At this point, the samples were etched in Kellers reagent for 20 seconds followed by immersion in concentrated nitric acid ( $\text{HNO}_3$ ) for five seconds. The samples were again etched in Kellers solution for 20 seconds followed by dipping in concentrated  $\text{HNO}_3$  for six to seven seconds. The samples were then rinsed in ethanol and dried [Ref. 24]. Metallography was then conducted by using a Zeiss ICM 405 optical microscope equipped with a 35mm camera.

#### IV. RESULTS AND DISCUSSION

##### A. MICROSTRUCTURAL CONDITION PRIOR TO ROLLING

Optical microscopy was conducted on material which had been solution treated for eight hours at 540 °C, forged to 25.4 mm and again annealed at 540 °C for four hours. This represents the condition prior to rolling. The microstructure consists of a mixture of elongated grains of large aspect ratio and more nearly equiaxed grains as shown in the micrograph of Figure 5. The equilibrium phases  $T_1$  and  $T_2$ , with solvi temperatures of 520 °C and 460 °C respectively, are not evident in this microstructure as a result of solution treatment. Some small uniformly distributed  $Al_3Zr$  particles as well as some slightly larger dark etching particles on grain boundaries are visible in this micrograph. These are likely to be inclusions. The elongation of grains in Figure 5 indicates the original rolling direction of the billet. This suggests that the hot forging has not introduced sufficient strain energy to lead to nucleation and growth of new grains through the structure. Instead some new grains have formed while the boundaries of others have been pinned by second phase particles.

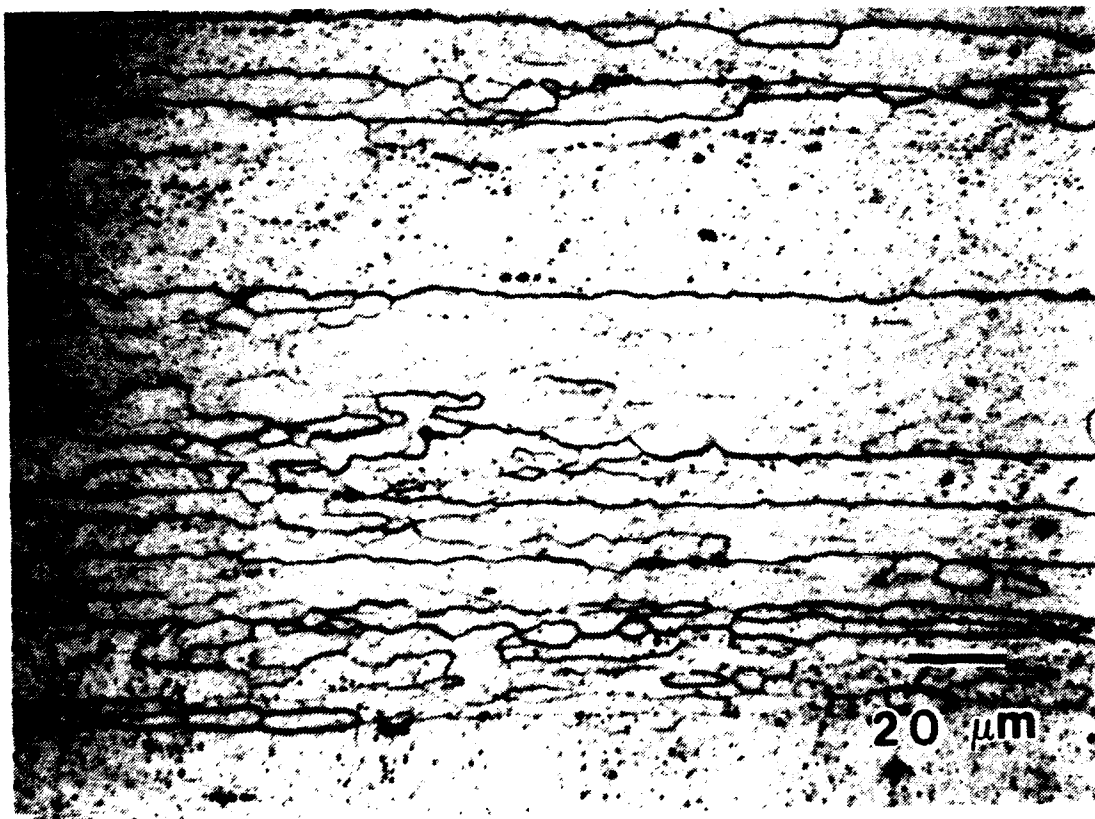
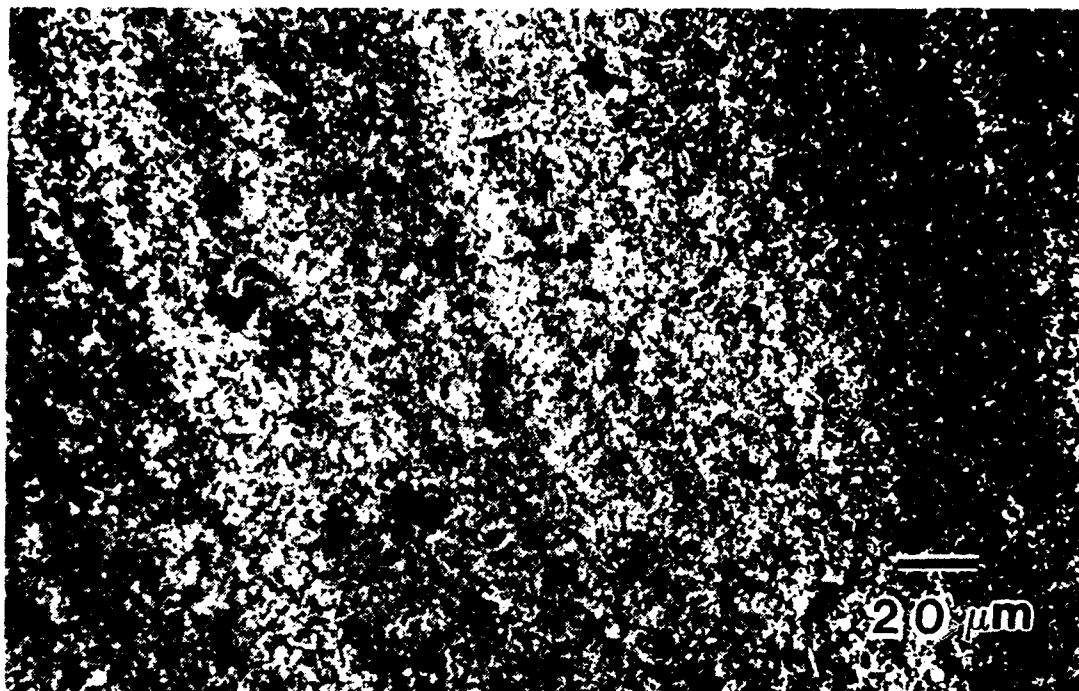


Figure 5. Long Transverse Optical Micrograph Of Alloy 2090 Following Solution Treatment At 540 °C For 8 Hours, Forged To 25.4mm At 480 °C, Annealed For 4 Hours At 540 °C And Quenched In Cold Water.

## B. MICROSTRUCTURAL CONDITION AFTER ROLLING

Optical micrographs of Al-2090 following warm rolling at 300°C to a true strain of 3.36, 2.60 at higher rolling speed and to 2.60 at lower rolling speed are shown in Figures 6, 7, and 8, respectively. In all three cases, warm rolling at 300°C with reheating intervals of 30 minutes between rolling passes has resulted in a fine second phase precipitate distributed in the microstructure. The higher rolling strain or rolling speed has not made appreciable difference in microstructure at this level of magnification. The TMP used has produced uniform microstructure with an intermetallic phase, likely  $T_2$  being the predominate precipitate. Groh [Ref. 7] has shown through TEM that, at the end of warm rolling, the precipitated  $T_2$  resides at triple junctions in the microstructure. Also deformation results in a diminished apparent volume fraction of  $T_1$  ( $Al_2-Cu-Li$ ), while the amount of  $T_2$  ( $Al_6-Cu-Li_3$ ) precipitate appears to increase. In micrographs of rolled surface (Figures 6a, 7a, and 8a) unsoluble inclusions are also evident.

(a)



(b)



Figure 6. Rolled Surface Section (a) And Long Transverse Section (b) Optical Micrographs Of Alloy 2090 Following Rolling At 300 °C To A True Strain Of 3.36 With 30 Minutes Reheating Intervals Between Passes.

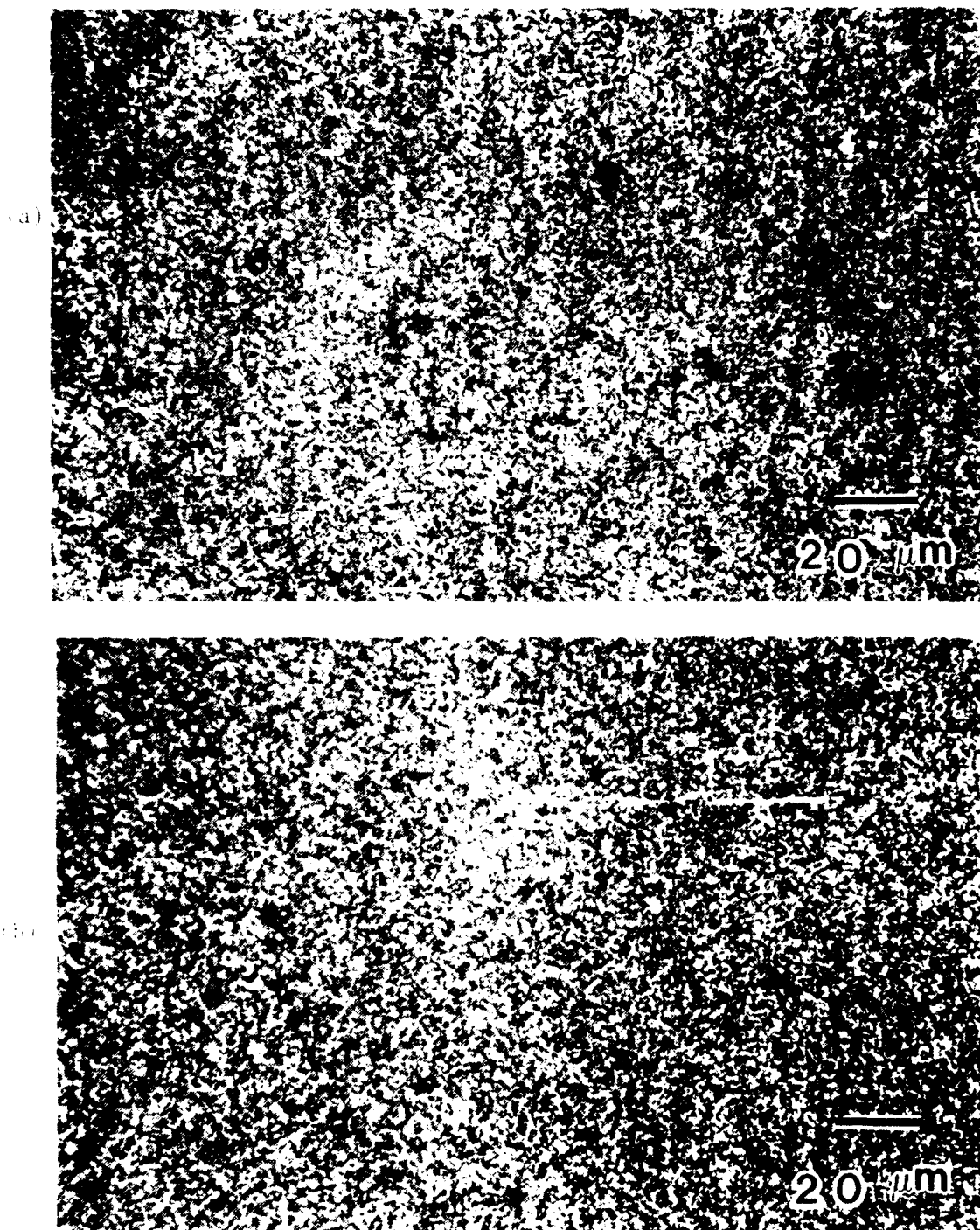


Figure 7. Rolled Surface Section (a) And Long Transverse Section (b) Optical Micrographs Of Alloy 2099 Following Rolling At 300 °C To A True Strain Of 2.60 With 30 Minutes Reheating Intervals Between Passes At Higher Rolling Speeds.

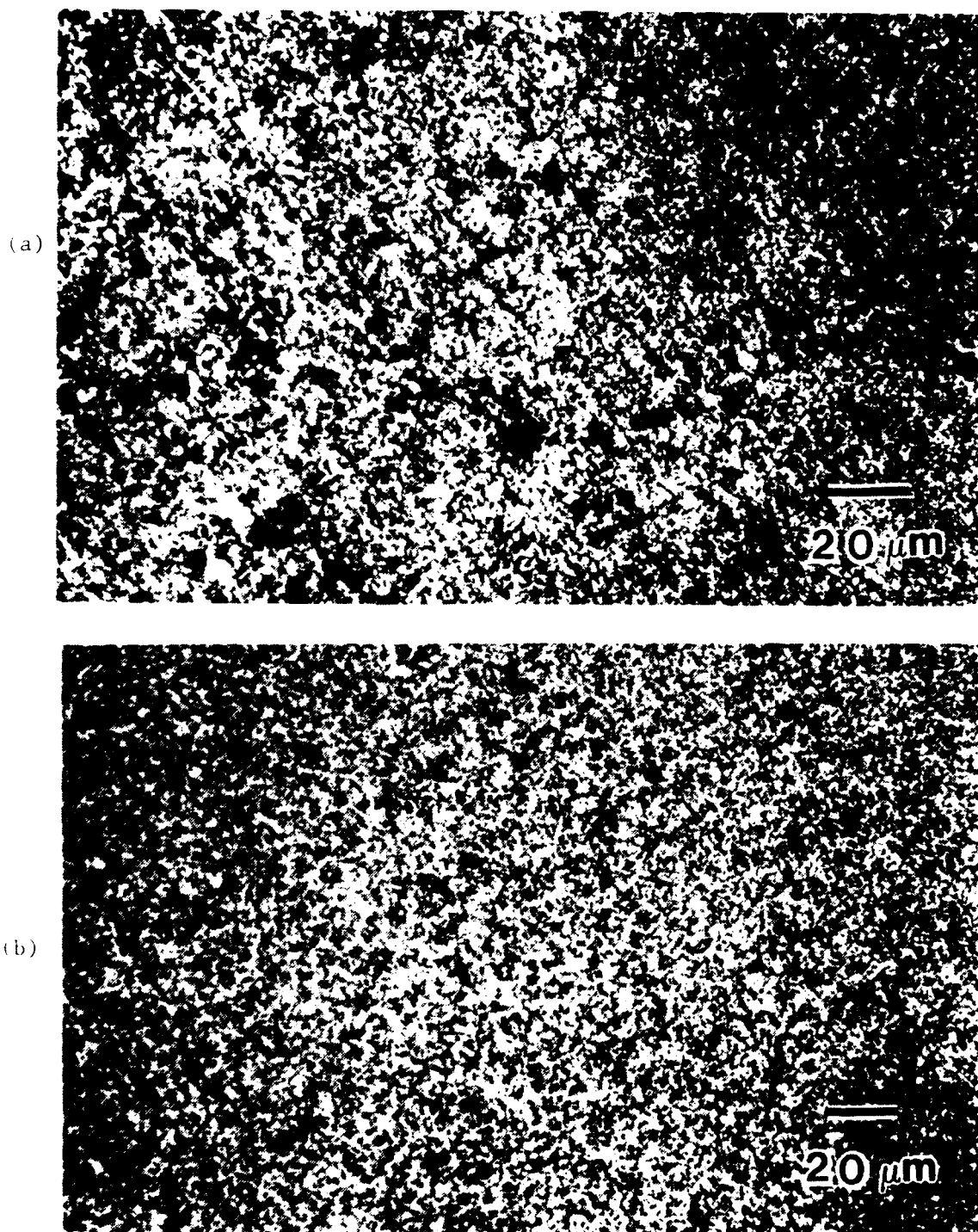


Figure 8. Rolled Surface Section (a) And Long Transverse Section (b) Optical Micrographs Of Alloy 2090 Following Rolling At 300 °C To A True Strain Of 2.60 With 30 Minutes Reheating Intervals Between Passes At Lower Rolling Speeds.



Figure 9. Long Transverse Section Optical Micrograph Of Alloy 2090 Specimen Following Rolling At 300 °C To A True Strain Of 3.36 With 30 Minutes Reheating Intervals Between Passes And Annealing At 540 °C For 10 Minutes.



The micrograph of Figure 9 shows the microstructure of material annealed at 540°C for ten minutes, at the end of warm rolling to a true strain of 3.36. This also represents the base line condition of the material comparable to that of Figure 5. A slight difference in the presence of phases is due to relatively shorter annealing period, in this case. Here, in addition to insoluble inclusions and Al<sub>3</sub>Zr particles (also insoluble at 540°C), undissolved precipitates, most likely T<sub>1</sub> due to its relatively higher solvus temperature and the short heating interval, can also be seen.

#### C. MECHANICAL PROPERTIES

Mechanical properties of Al-2090 were examined considering final rolling strain and rolling speed as primary variables. This was accomplished by testing of the processed material over a range of temperatures and strain rates. Due to the emergence of similar microstructure at the end of TMP, in all cases (i.e., in material rolled to 3.36 true strain, 2.60 true strain at higher rolling speed and 2.60 true strain at lower rolling speed), the elongations obtained were of the same order. Moderate ductilities were obtained between 370°C and 430°C and strain rates of  $6.67 \times 10^{-4} \text{ s}^{-1}$  and

$6.67 \times 10^{-3} \text{ s}^{-1}$ , irrespective of final rolling strain or the rolling speed. The results of the mechanical testing are summarized graphically in Figures 10-15 and in tabulated form in Table A-1 of Appendix A.

It can be seen from these results that the ductilities were relatively low at lower temperatures and again decreased at temperatures above  $430^\circ \text{C}$ . As mentioned in Section A of this chapter, a reasonably refined microstructure was obtained at the end of TMP (Figures 6, 7, and 8). This microstructure would suggest lower ductilities at relatively low temperatures due to the fact that smaller grains are more resistant to flow at lower temperatures [Ref. 22]. The drop in elongations at higher temperatures, then, is likely due to the coarsening of microstructure.

The peak ductility of 240 percent was achieved in a material rolled to true strain of 3.36 and subsequently tested in tension at a strain rate of  $6.67 \times 10^{-4} \text{ s}^{-1}$  at  $430^\circ \text{C}$ . In a material rolled to true strain of 2.60 at higher rolling speed, the highest value of elongation, 215 percent, was obtained in testing at a strain rate of  $6.67 \times 10^{-3} \text{ s}^{-1}$  at  $400^\circ \text{C}$ . Similarly the value of 226 percent elongation was attained in material rolled to 2.60 true strain at lower rolling speed and then tested at  $370^\circ \text{C}$ . These values are so close that a clear distinction of variable parameters can not be established.

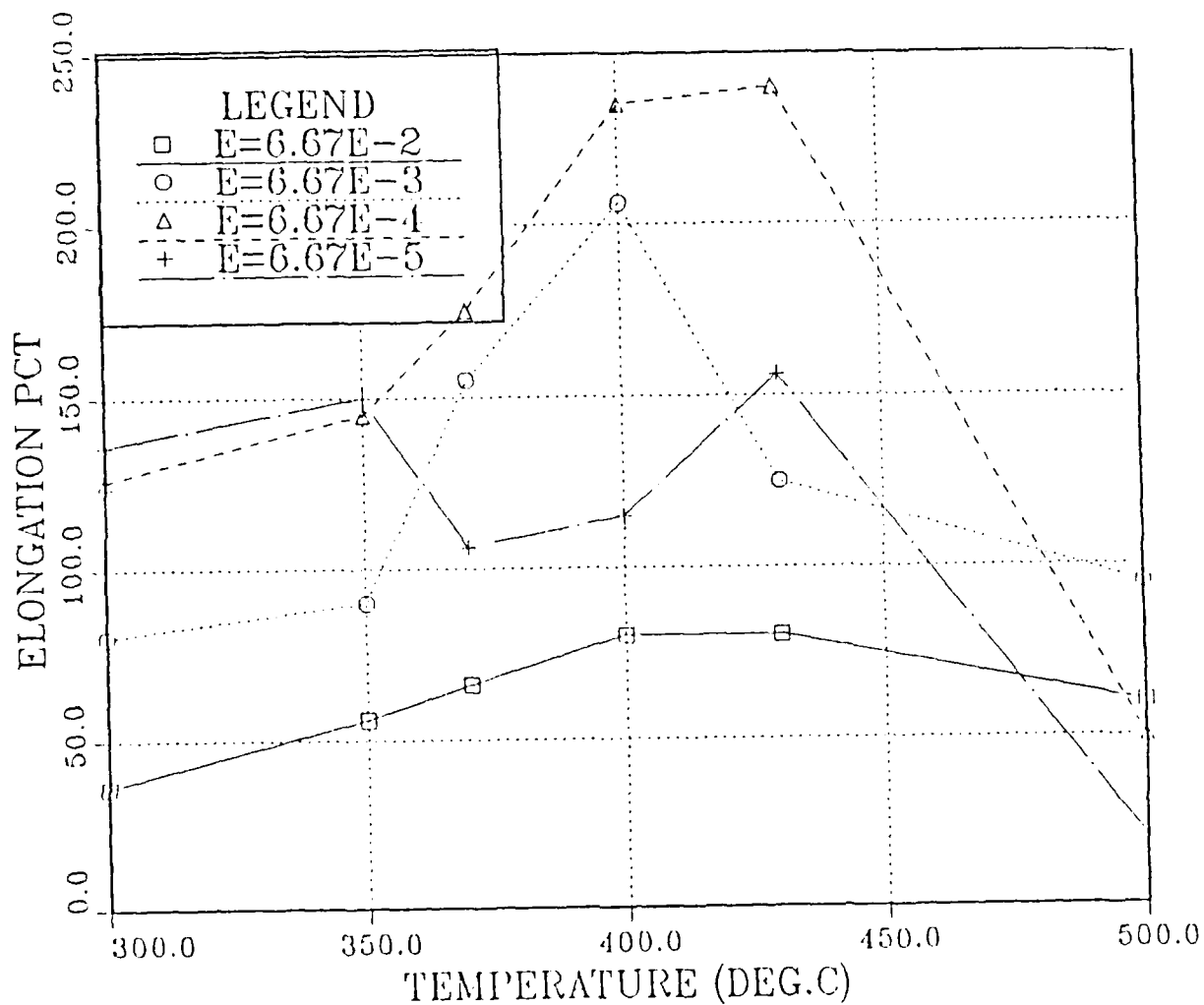


Figure 10. Ductility vs. Tensile Test Temperature For Various TMP Schedules Shown In The Legend. The Material Was Rolled In The Original Plate Longitudinal Direction With True Strain Of 3.36.

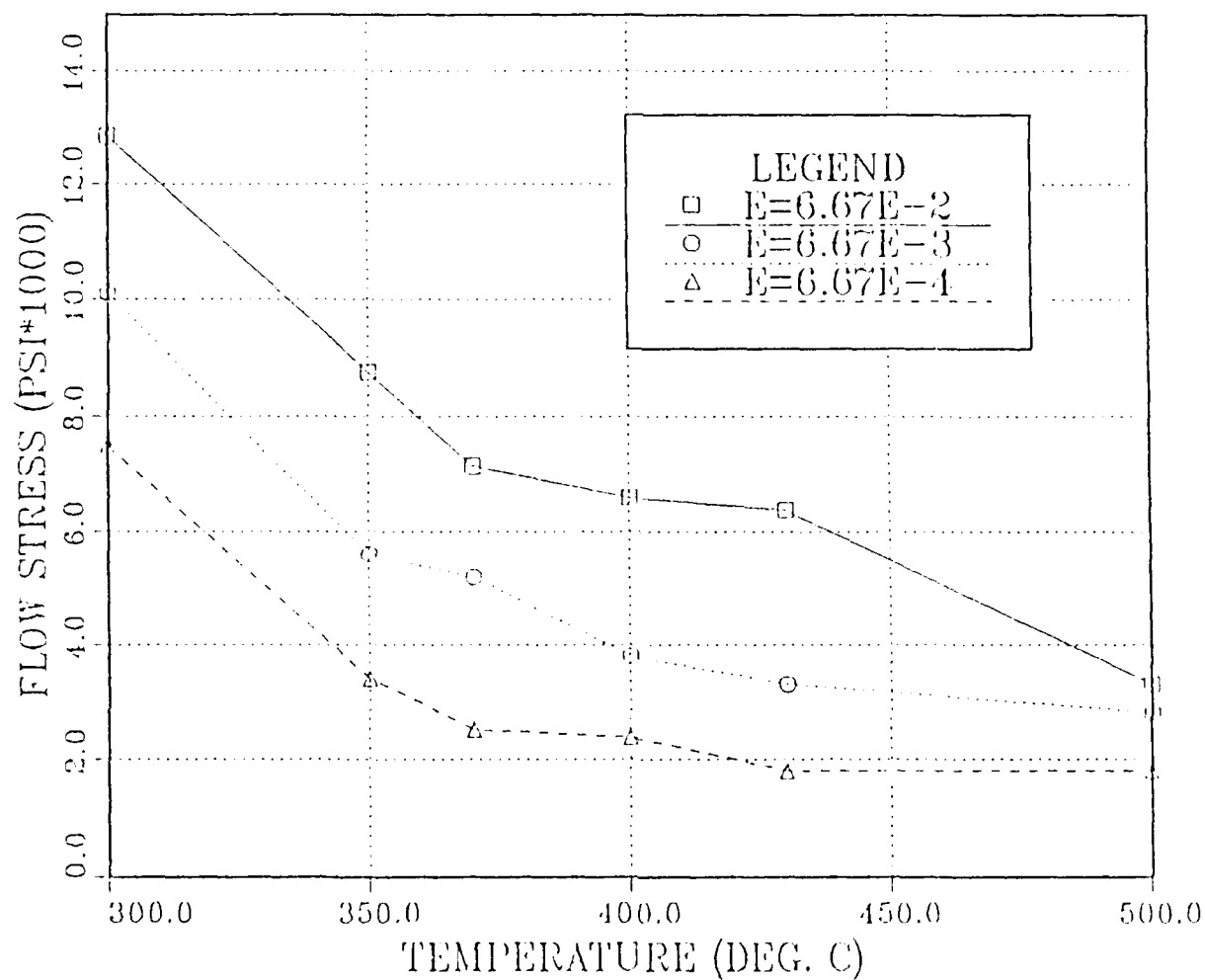


Figure 11. Flow Stress AT Strain Of 0.1 In/In.  
The Material Was Rolled In The Original  
Longitudinal Plate Direction To A  
Rolling Strain Of 3.36.

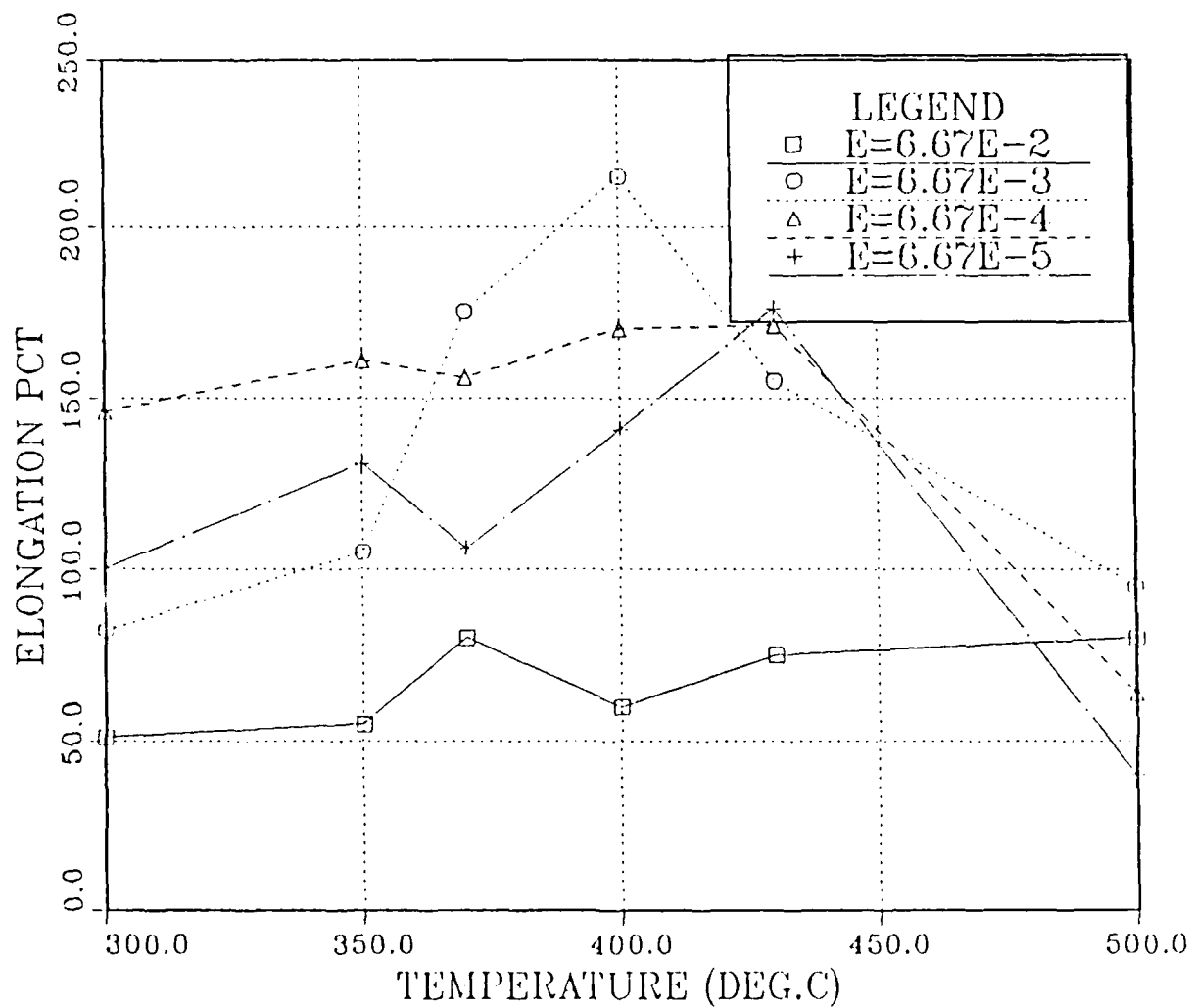


Figure 12. Ductility vs. Tensile Test Temperature For Various TMP Schedules Shown In The Legend. The Material Was Rolled In The Original Plate Longitudinal Direction With True Strain Of 2.60 at High Rolling Speed.

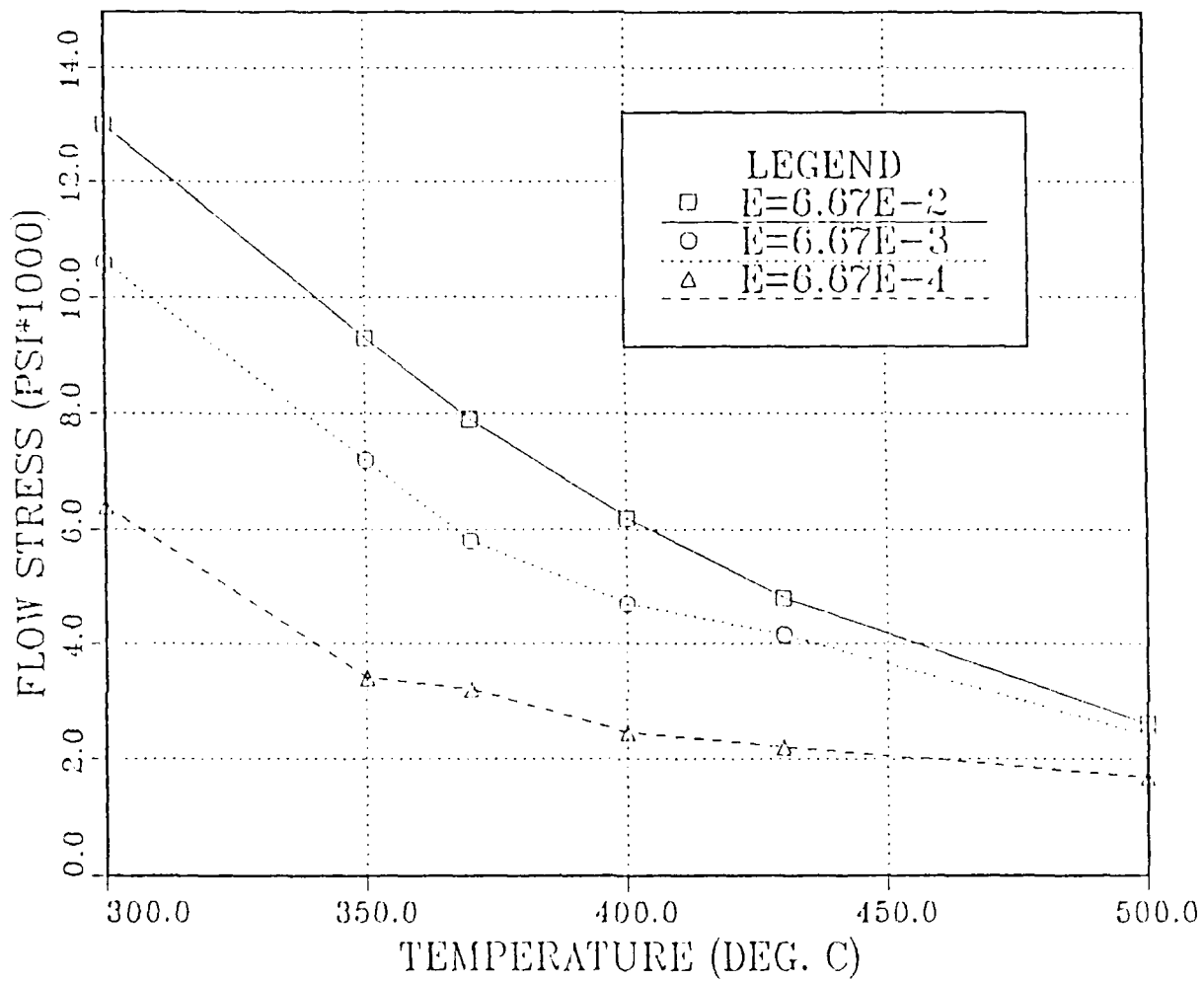


Figure 13. Flow Stress At Strain Of 0.1 In/In.  
The Material Was Rolled In The Original  
Longitudinal Plate Direction To A Rolling  
Strain of 2.60 At Higher Rolling Speed.

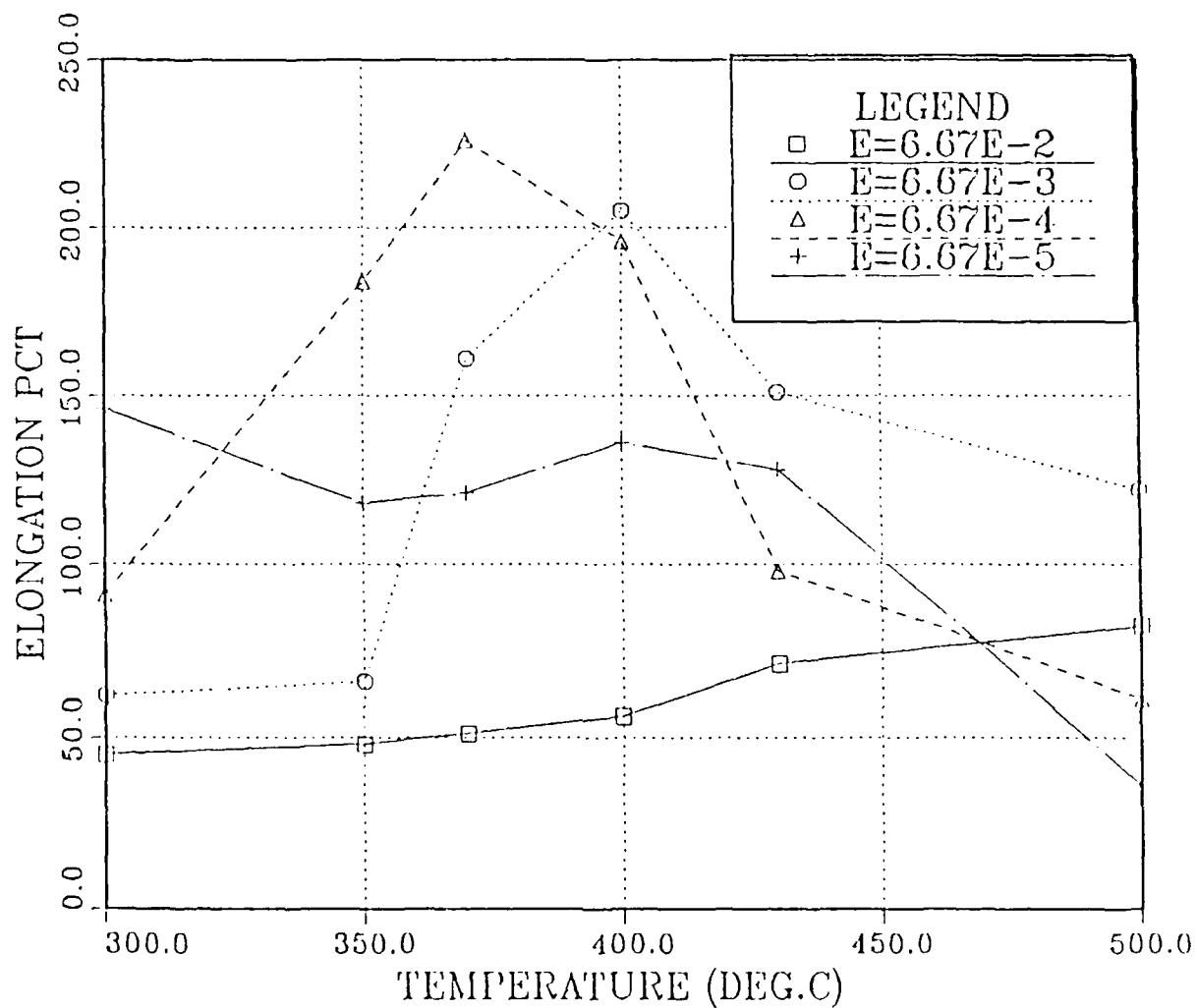


Figure 14. Ductility vs. Tensile Test Temperature For Various TMP Schedules Shown In The Legend. The Material Was Rolled In The Original Plate Longitudinal Direction With True Strain Of 2.60 At Lower Rolling Speed

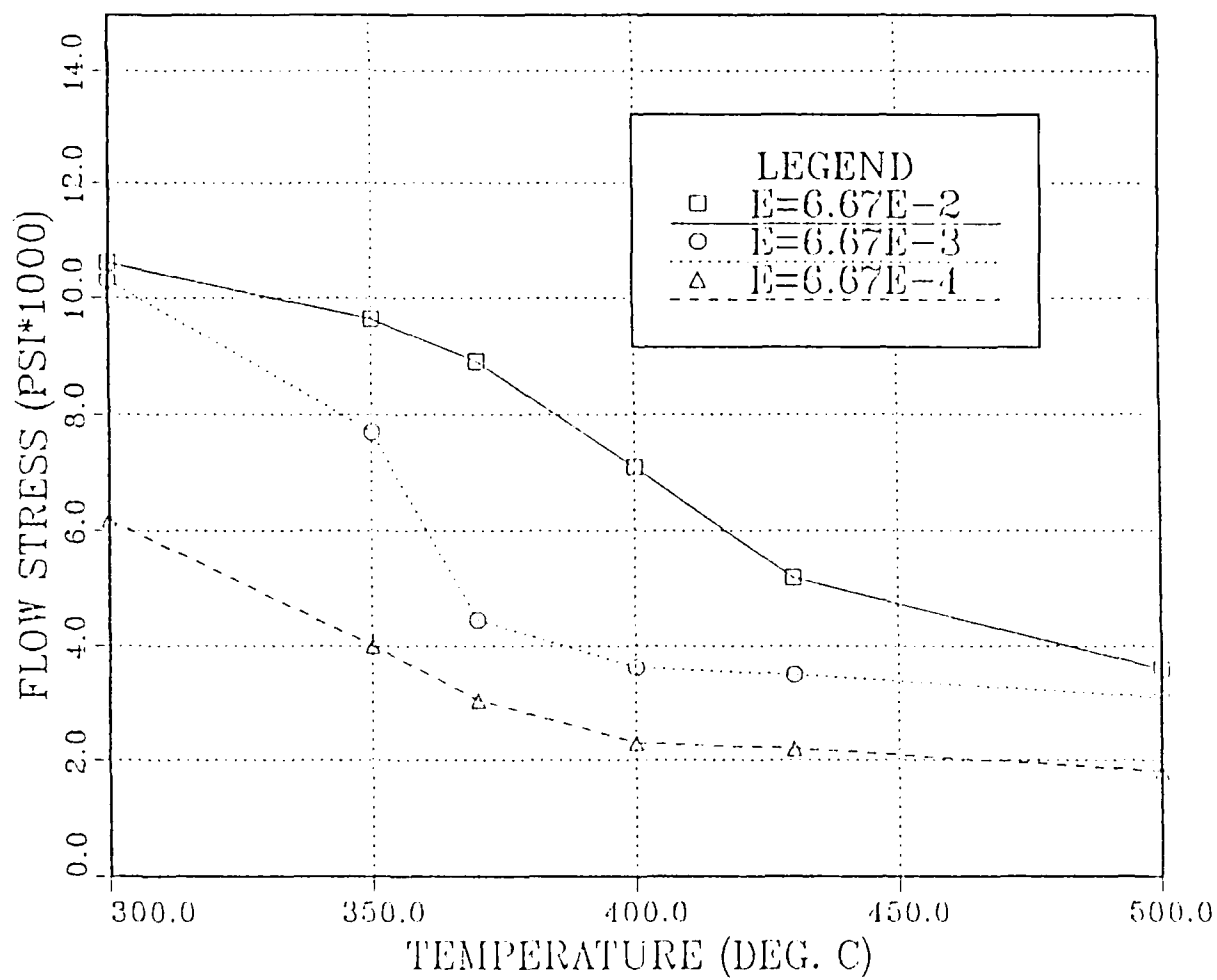


Figure 15. Flow Stress At Strain Of 0.1 In/In.  
The Material Was Rolled In The Original  
Longitudinal Plate Direction To A Rolling  
Straiun Of 2.60 At Lower Rolling Speed.



During the tensile tests, the flow stress decreases with decreasing strain rates as can be seen from Figures 11, 13, and 15. Although flow stress values at test temperatures above 430°C are very low in all cases at all strain rates, the value of strain rate sensitivity coefficient obtained was not of high enough magnitude. The highest value of  $m$  obtained was of the order of  $\sim 0.3$  at 430°C in material rolled to true strain of 3.36 (Figure 16). The value of this coefficient dropped at temperatures above and below 430°C in this case. This is consistent with the results graphically represented in Figure 10 and tabulated in Table A-1 of Appendix A.

Normally, the value of  $m$  increases with rising temperature. However,  $m$  is also a function of microstructure of the material, usually attaining values of 0.5 in fine grained, recrystallized microstructures when high-angle boundaries are present. Hence the lower values of  $m$  above 430°C is attributed to coarser grains and the failure to attain higher angle boundaries in processing.

The fact that the coarser grain structure is less ductile (lower  $m$  value) than fine grain structure at elevated temperatures can be observed in the data of Figures 17 and 18. The tensile tests conducted on specimens annealed at 540°C for 10 minutes, prior to tension testing resulted in much lower ductilities as

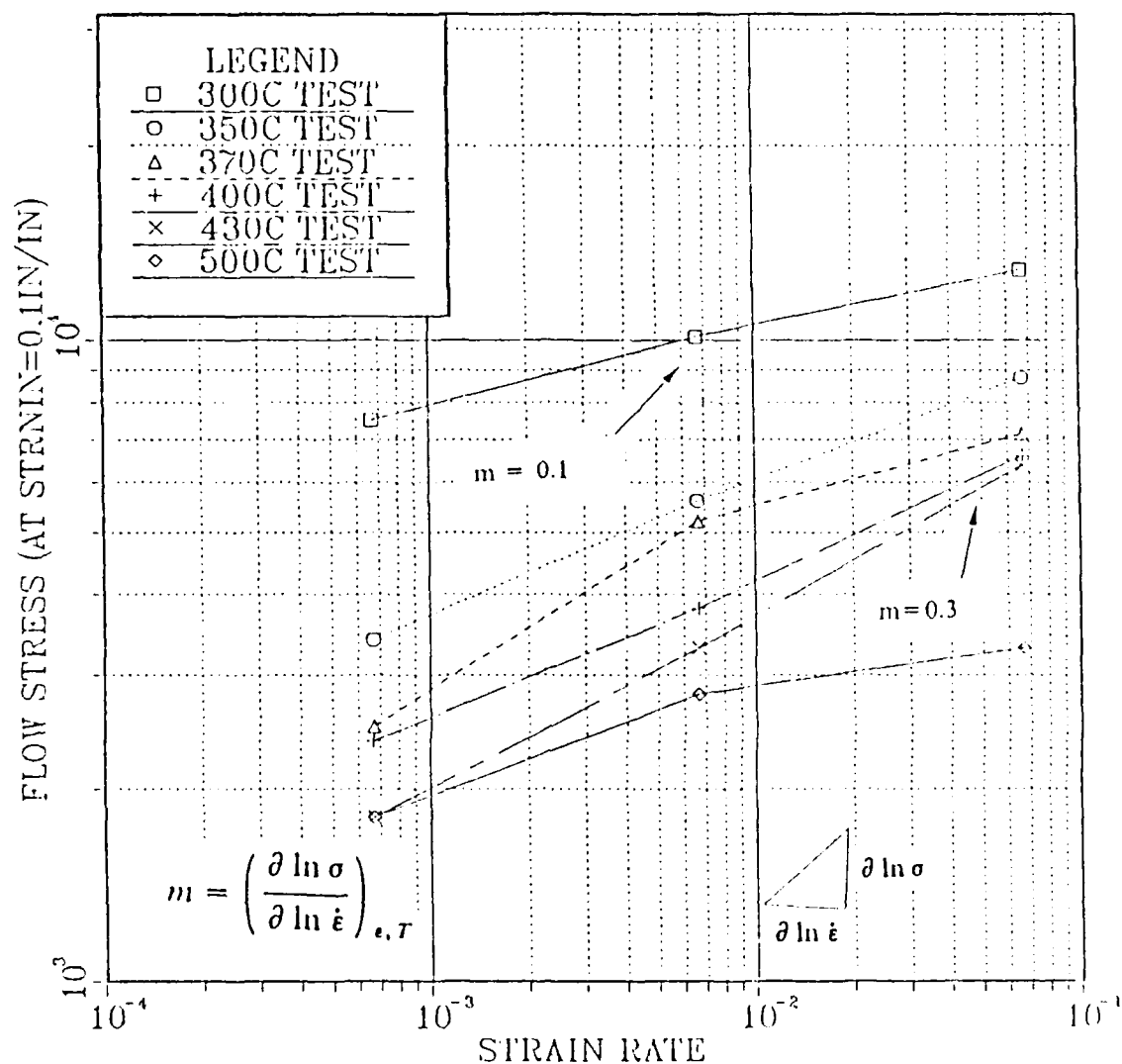


Figure 16. Flow Stress vs. Strain Rate At Strain Of 0.1 In/In For Material Rolled To 3.36 True Strain.

compared to as rolled specimens. The reason for this was the coarser grain structure of annealed material. The microstructure of as rolled material tested at 500 °C also resulted in coarser grains, resulting in ductility of the same order of annealed material.

Important outcome of these results is that the TMP utilized in this research work failed to achieve boundaries of sufficient misorientation and ability to resist grain growth at higher test temperatures. The cavitation at temperatures above 400 °C was also not suppressed due to which premature fracture of material resulted, consequently producing low ductilities.

Finally, Figures 17 and 18 emphasize that the microstructures developed by this TMP do result in enhancement of ductility in comparison to that of an initially annealed, course-grained condition. Thus, as also concluded by Groh [Ref. 7], the attainment of boundaries of sufficient misorientation in conjunction with resistance to coarsening should result in further enhancement of ductility. However, increased rolling strain with this particular material has not as yet produced the desired result.

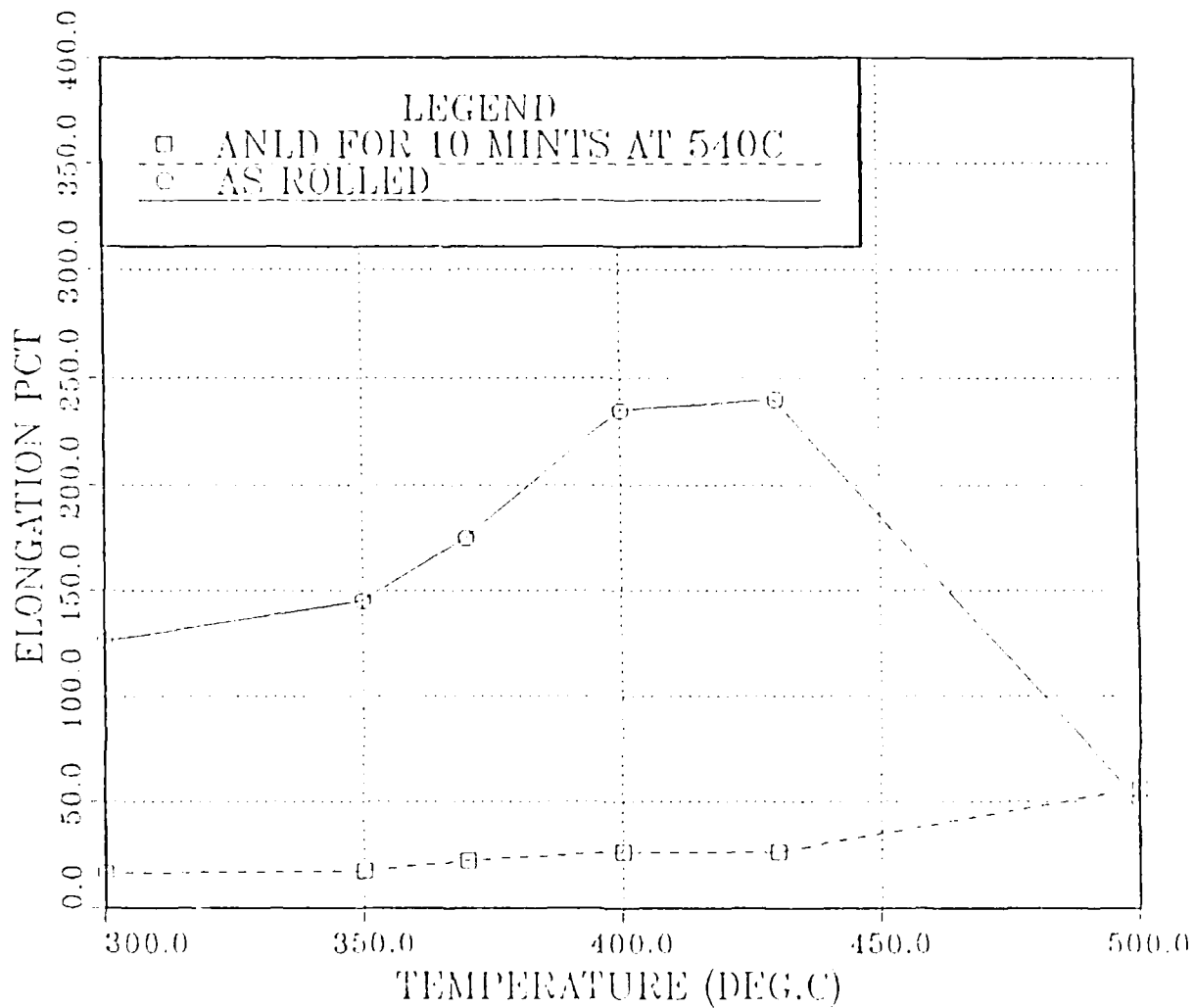


Figure 17. Ductility vs. Temperature For Various TMP Schedules Shown In The Legend. The Material was rolled to a true strain of 3.36 In The Original Longitudinal Plate Direction.

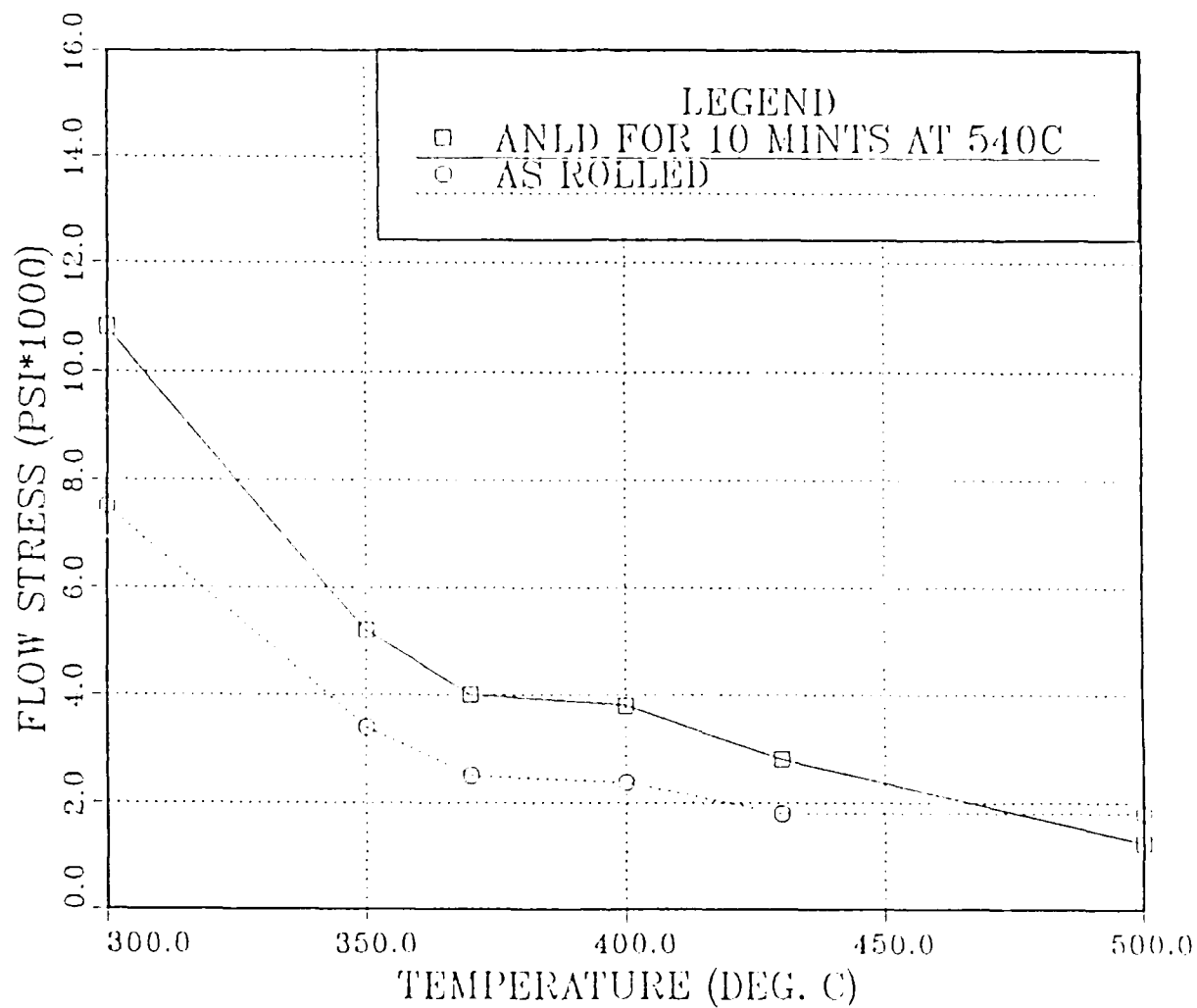


Figure 18. Comparison Of Flow Stress AT A Strain Rate Of  $6.67 \times 10^{-4} \text{ s}^{-1}$ . The Material Was Rolled To A True Strain Of 3.36.

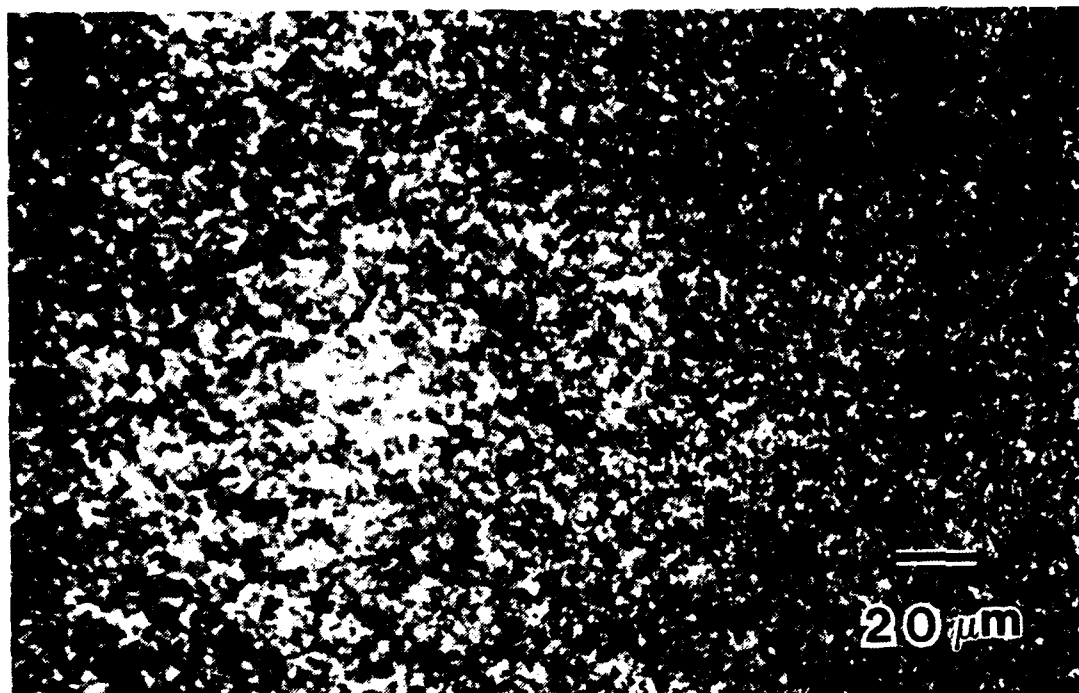
#### D. EFFECT OF DEFORMATION ON MICROSTRUCTURE

As mentioned in the previous section, the highest value of elongation was obtained in material rolled to true strain of 3.36, tested at 400 °C at a strain rate of  $6.67 \times 10^{-4} \text{ s}^{-1}$ . The microstructure present in this sample is shown in Figure 19. The micrograph of Figure 19b represents the effect of heating only of the as-rolled condition.

It can be seen in Figure 19a that the microstructure of deformed section, i.e. the gage section, has coarsened somewhat and predominant  $T_2$  phase is clearly evident in the micrograph. The relatively low temperature of 400 °C has not resulted in extensive microstructural coarsening and the material has shown good elongation.

Microscopy on a sample tested at 500 °C revealed totally different microstructure, as shown in Figure 20. Large grains can be seen in grip section (Figure 20b) whereas highly elongated grains along with some equiaxed smaller grains are evident, in the deformed gage section (Figure 20a). The presence of smaller, equiaxed grains suggest recrystallization and growth upon straining at 500 °C. Also noteworthy is the presence of cavitation on the grain boundaries, and this likely is the cause of premature failure at elevated temperatures during tensile tests.

(a)



(b)



Figure 19. Long Transverse Gage Section (a) And Grip Section (b) Optical Micrographs Of Alloy 2090 Following Tensile Test Conducted At 400 °C At Strain Rate of  $6.67 \times 10^{-4} \text{ s}^{-1}$ . The Material Was Rolled At 300 °C. To A True Strain of 3.36 With 30 Minutes Reheating Intervals Between Passes. The Microstructure Is Similar To As Rolled Conditions And Coarsening Has Not Taken Place.

To provide a basis for comparison, material warm rolled to true strain of 3.36 was annealed at 540 °C for ten minutes prior to conducting the subsequent tensile tests at various temperatures. This reheating produced much coarser initial structure as shown previously in Figure 9. The micrographs of Figure 21 represents the gage and grip sections, respectively, of this material following tension testing at 400 °C and a strain rate of  $6.67 \times 10^{-4} \text{ s}^{-1}$ . Here, precipitation during heating and straining is evident and elongation of grains in the gage section is also apparent. The microstructure is homogeneous with no sign of cavitation. Much reduced ductilities under these conditions are the direct result of the coarse grain structure; the grain elongation certainly reflects dislocation deformation and lower ductility. Thus, refined microstructures consisting only of recovered subgrains rather than recrystallized grains are sufficient to enhance ductility, although grains with high-angle boundaries are necessary for extensive superplasticity.

Figure 22 represents the gage and grip section, respectively, of the same annealed material but now tested at 500 °C. These micrographs also reflect the much coarser, initial microstructure, but now along with extensive cavitation in the necking region. The fracture surface of this sample is seen in profile at right in



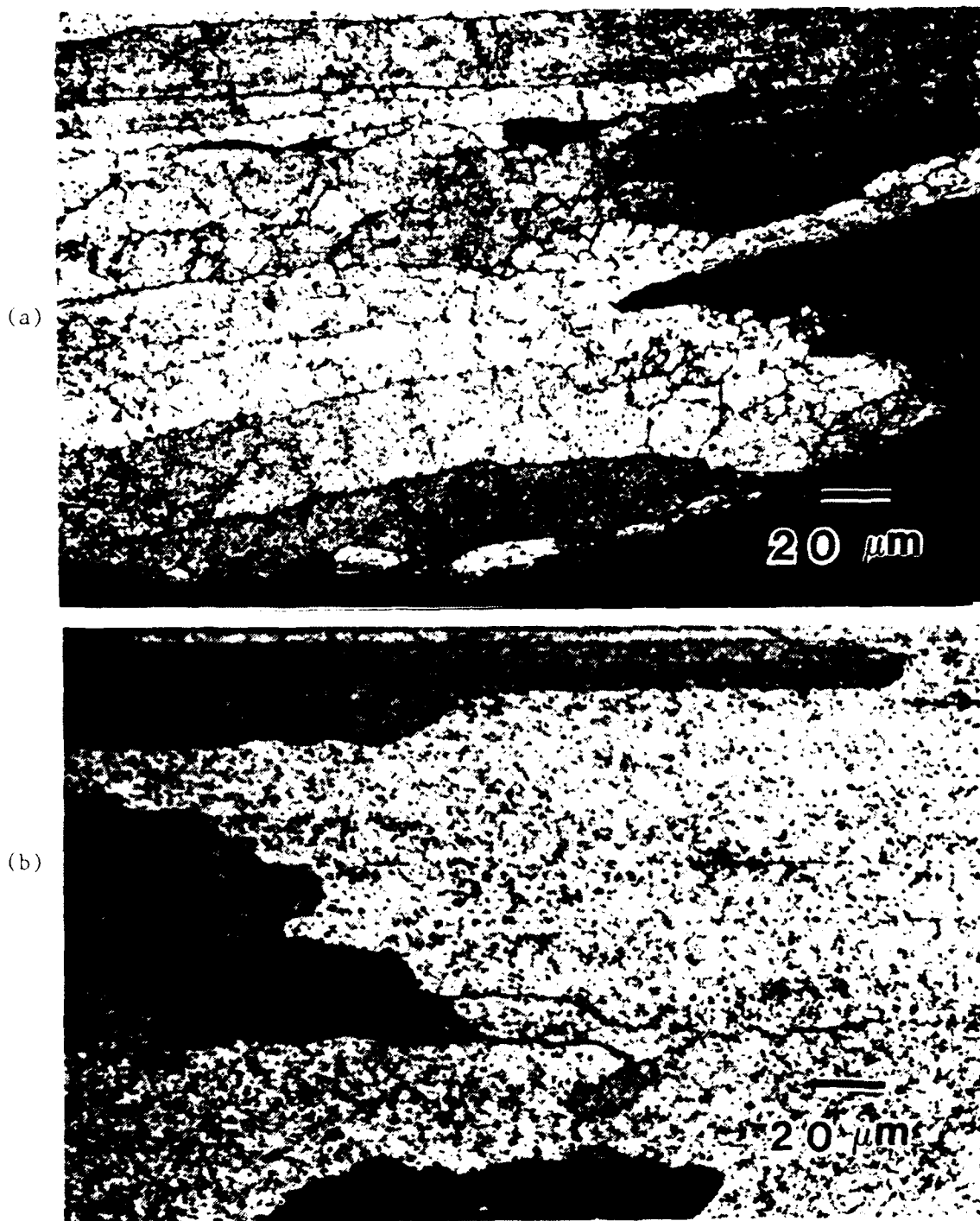


Figure 20. Long Transverse Gage Section (a) And Grip Section (b) Optical Micrographs Of Alloy 2090 Following Tensile Test Conducted At 500 °C At Strain Rate of  $6.67 \times 10^{-4} \text{ s}^{-1}$ . The Material Was Rolled At 300 °C. To A True Strain of 3.36 With 30 Minutes Reheating Intervals Between Passes. The Cavitation Along The Boundaries Is Very Clear AT 500 °C.

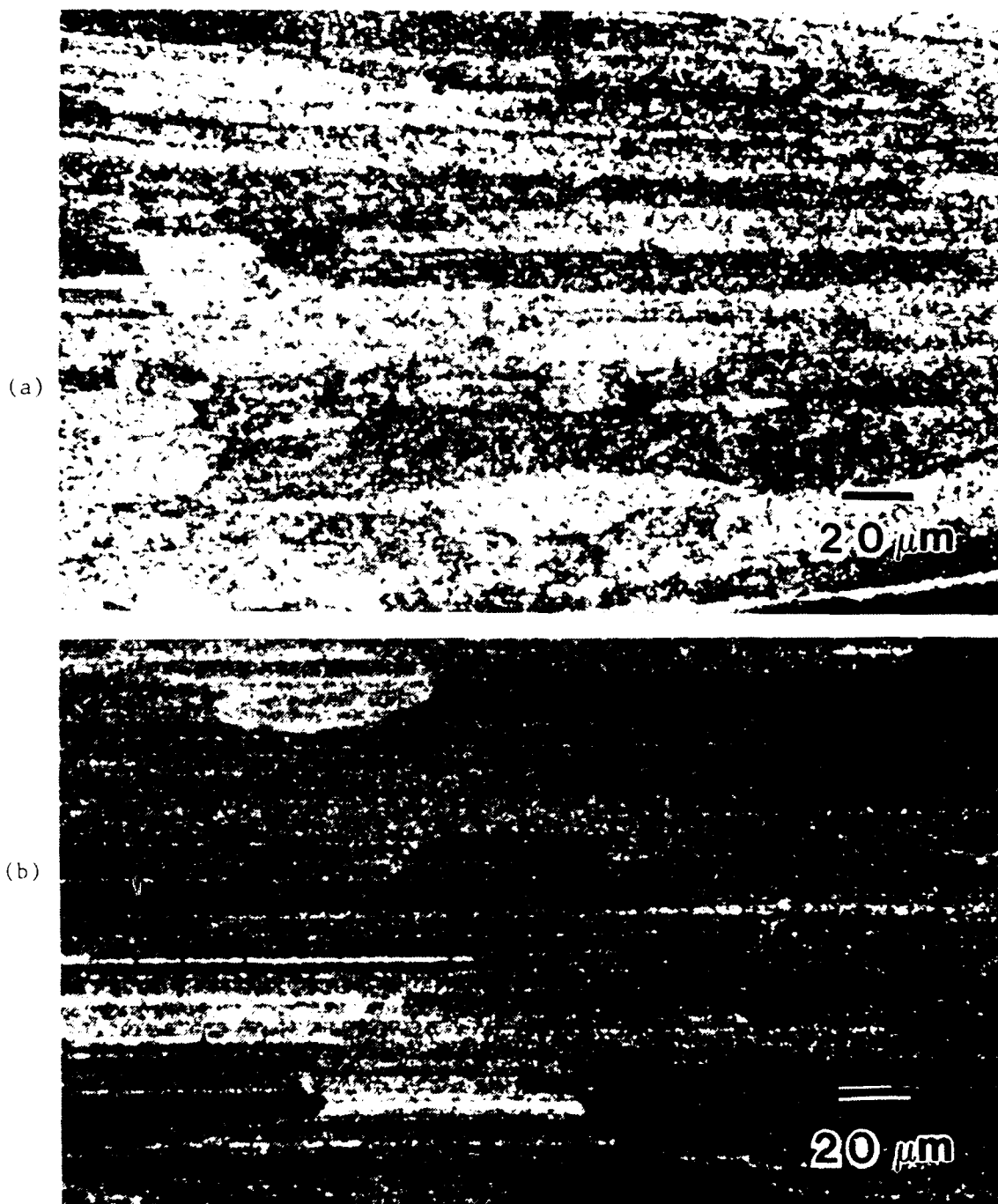


Figure 21. Long Transverse Gage Section (a) And Grip Section (b) Optical Micrographs Of Alloy 2090 Following Tensile Test Conducted At 400°C At Strain Rate of  $6.67 \times 10^{-4} \text{ s}^{-1}$ . The Material Was Rolled At 300°C To A True Strain of 3.36 With 30 Minutes Reheating Intervals Between Passes. The Specimen Was Annealed At 540°C For 10 Minutes Before Conducting Tensile Tests.

Figure 22a, once again clearly indicates the premature failure of material on the grain boundaries. It is evident from Figure 20a and 22a that alloy 2090 is very prone to grain boundary separation and cavitation at elevated temperatures. This may be due to various factors including, the presence of impurities such as Fe, Na and K.



Figure 22. Long Transverse Gage Section (a) And Grip Section (b) Optical Micrographs Of Alloy 2090 Following Tensile Test Conducted At 500°C At Strain Rate of  $6.67 \times 10^{-4} \text{ s}^{-1}$ . The Material Was Rolled At 300°C. To A True Strain of 3.36 With 30 Minutes Reheating Intervals Between Passes. The Specimen Was Annealed At 540°C For 10 Minutes Before Conducting Tensile Tests. Concentration Of Cavitation On Grain Boundaries Is Clearly Evident In Gage Section, Particularly Towards The Necking.

#### E. SUMMARY

The sequence of precipitation and development of microstructure in aluminum alloy 2090 is not fully understood as yet. The  $T_2$  phase may play a similar role to the  $\beta$  phase in Al-Mg-X alloys in achieving superplastic response in Al-2090. In this research initial homogenization, reasonably even distribution of precipitates and finally a fine microstructure was obtained for all TMP conditions. Despite this the ductilities obtained were considered much below the anticipated values. In fact, the strain rate sensitivity coefficients were  $\sim 0.3$  at best and thus the reduced ductilities were consistent with this aspect of the material. This likely reflects incomplete conversion of the microstructure to a fine grained structure with high angle grain boundaries.

It was previously suggested [Ref. 7] that higher accumulated rolling strain, producing a higher density of dislocations, will promote superplasticity by creating even finer microstructure through continuous recrystallization. However, no improvement was observed either by increasing the overall rolling strain beyond true strain of 2.50 or the rolling speed. The micrographs of Figures 20 and 22 also suggested that at

higher test temperatures, the grain boundaries began to fail. Thus, processing failed to suppress the creation of cavitation at elevated temperatures. This phenomenon of excessive cavitation, particularly in the necking region, may have been the result of excessive impurity contents. The material was also unable to maintain the refined state of microstructure and the spontaneous grain growth at higher test temperatures, resulted in much reduced elongations.

## V. CONCLUSION

The conclusions of this study are drawn as follows:

(a) Warm rolling resulted in moderate superplastic response.

(b) Refined microstructure was obtained following TMP. However, TEM studies previously conducted, showed that such processing results in low angle grain boundaries which normally does not support extensive superplasticity.

(c) Optical micrography also revealed that development of coarser structure during the tests at elevated temperatures, became the cause of reduced or low elongations.

(d) Microstructure obtained at the end of TMP failed to suppress cavitation at elevated temperatures.

(e) In comparison with previous thesis work done at NPS, increased rolling strain beyond 2.50 and higher rolling speed did not improve the ductilities.

## VI. RECOMMENDATIONS

The following recommendations are made for following-up this study:

(a) Attain rolling strain of 2.50 through a rolling schedule in which the rolling speed is to be increased on every successive pass (as recommended by McQueen in Ref. 25). This type of rolling may provide finer microstructure with high angle grain boundaries.

(b) Obtain material with lowest acceptable impurity contents.



# APPENDIX A

## TABLE A-1

### SUMMARY OF DUCTILITY DATA

Processing Condition			Elongation (PCT.)					
Strain Rate	Rolling Strain	Rolling Speed	Test Temperature (C°)					
			300	350	370	400	430	500
$6.67 \times 10^{-2} \text{S}^{-1}$	3.36	High	36	56	66	80	80	60
$6.67 \times 10^{-3} \text{S}^{-1}$	3.36	High	80	90	155	206	125	95
$6.67 \times 10^{-4} \text{S}^{-1}$	3.36	High	126	145	175	235	240	50
$6.67 \times 10^{-5} \text{S}^{-1}$	3.36	High	136	150	106	115	156	20
$6.67 \times 10^{-4} \text{S}^{-1} *$	3.36	High	16	17	22	26	26	56
$6.67 \times 10^{-2} \text{S}^{-1}$	2.60	High	51	55	80	60	75	80
$6.67 \times 10^{-3} \text{S}^{-1}$	2.60	High	82	105	175	215	155	95
$6.67 \times 10^{-4} \text{S}^{-1}$	2.60	High	146	161	156	170	171	64
$6.67 \times 10^{-5} \text{S}^{-1}$	2.60	High	100	131	106	141	176	40
$6.67 \times 10^{-2} \text{S}^{-1}$	2.60	Low	45	48	51	56	72	82
$6.67 \times 10^{-3} \text{S}^{-1}$	2.60	Low	62	66	161	205	151	122
$6.67 \times 10^{-4} \text{S}^{-1}$	2.60	Low	91	184	226	196	98	61
$6.67 \times 10^{-5} \text{S}^{-1}$	2.60	Low	146	118	121	136	128	36

\* The samples were annealed at 540°C for ten minutes before conducting tensile tests.

APPENDIX B  
TENSILE TEST DATA

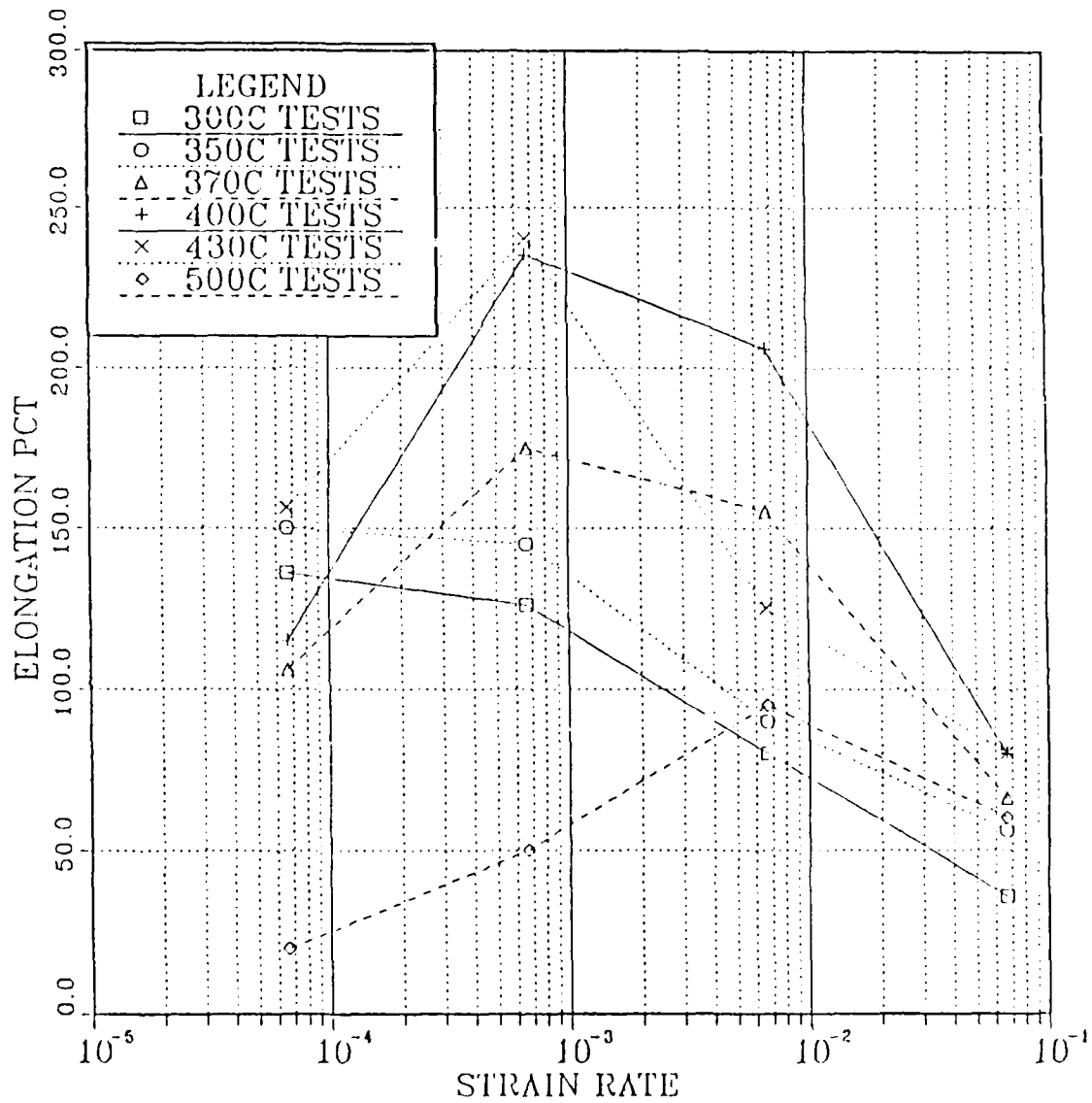


Figure B-1. Ductility vs. Strain Rate For Various TMP Schedules Shown In The Legend. The Material Was Rolled In The Original Plate Longitudinal Direction With True Strain Of 3.36.

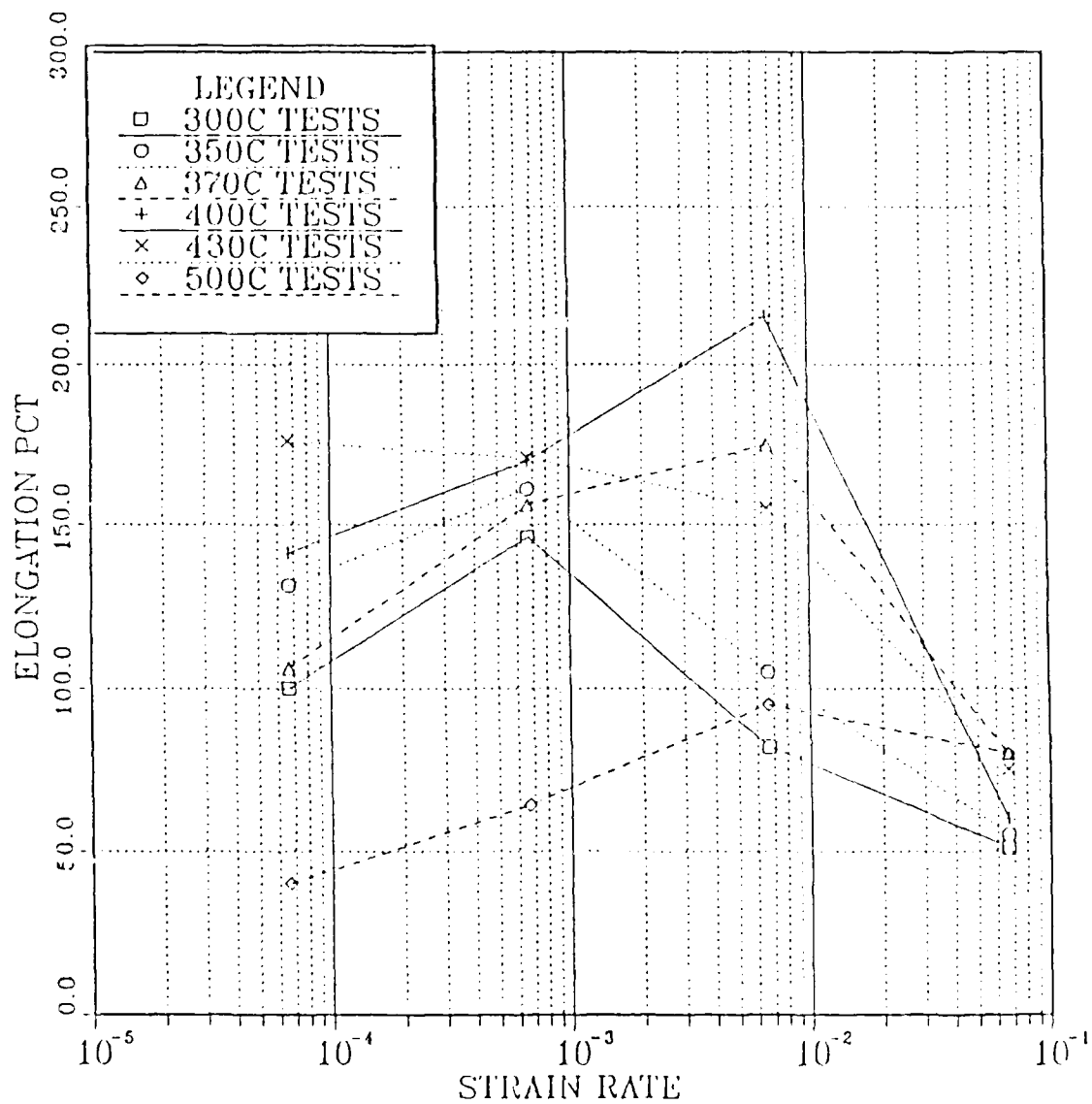


Figure B-2. Ductility vs. Strain Rate For Various TMP Schedules Shown In The Legend. The Material Was Rolled In The Original Plate Longitudinal Direction With True Strain Of 2.60 At Higher Rolling Speed

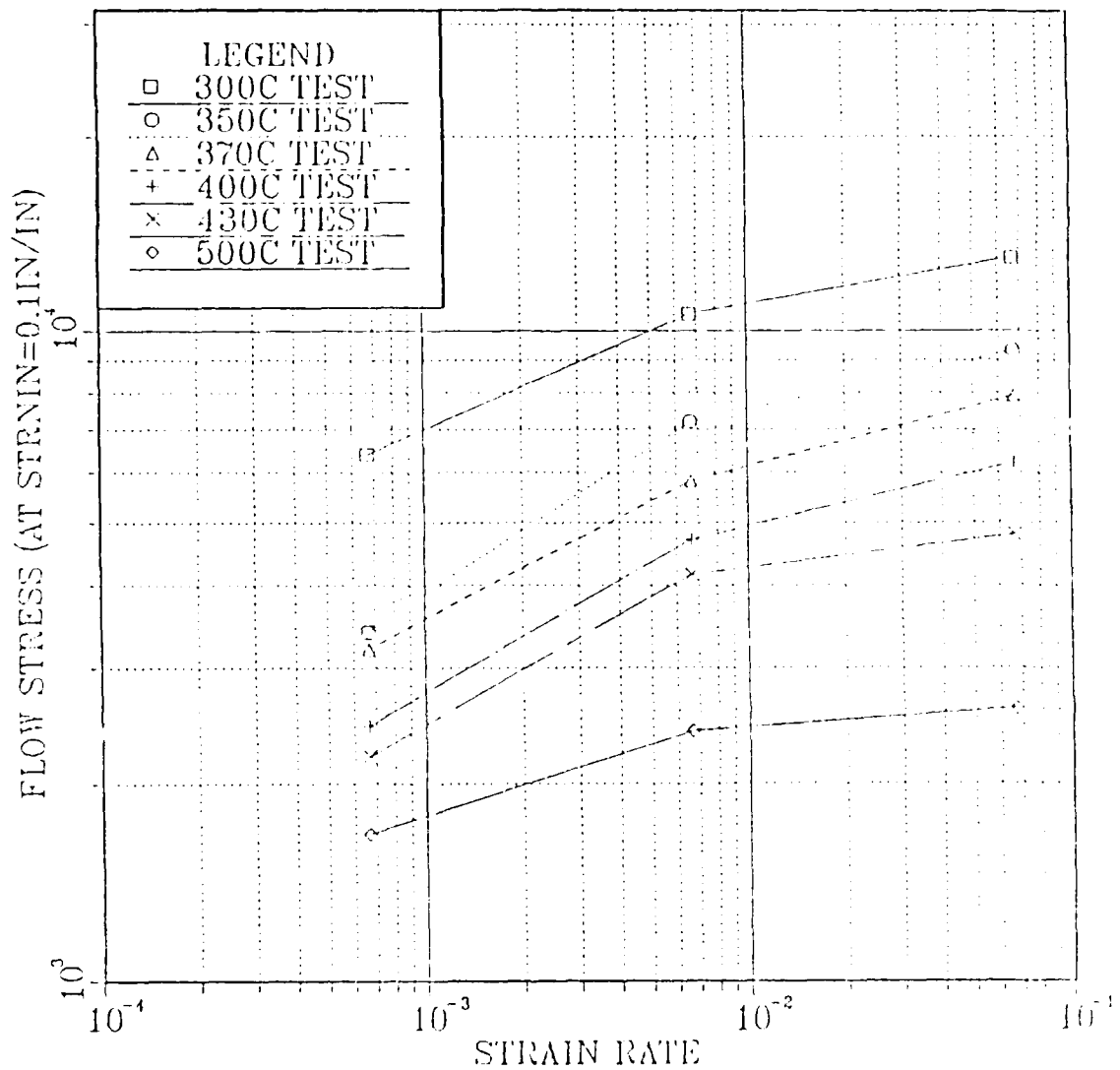


Figure B-3. Flow Stress vs. Strain At Strain Of 0.1  
For Material Rolled To 2.60 True Strain At  
Higher Rolling Speed.

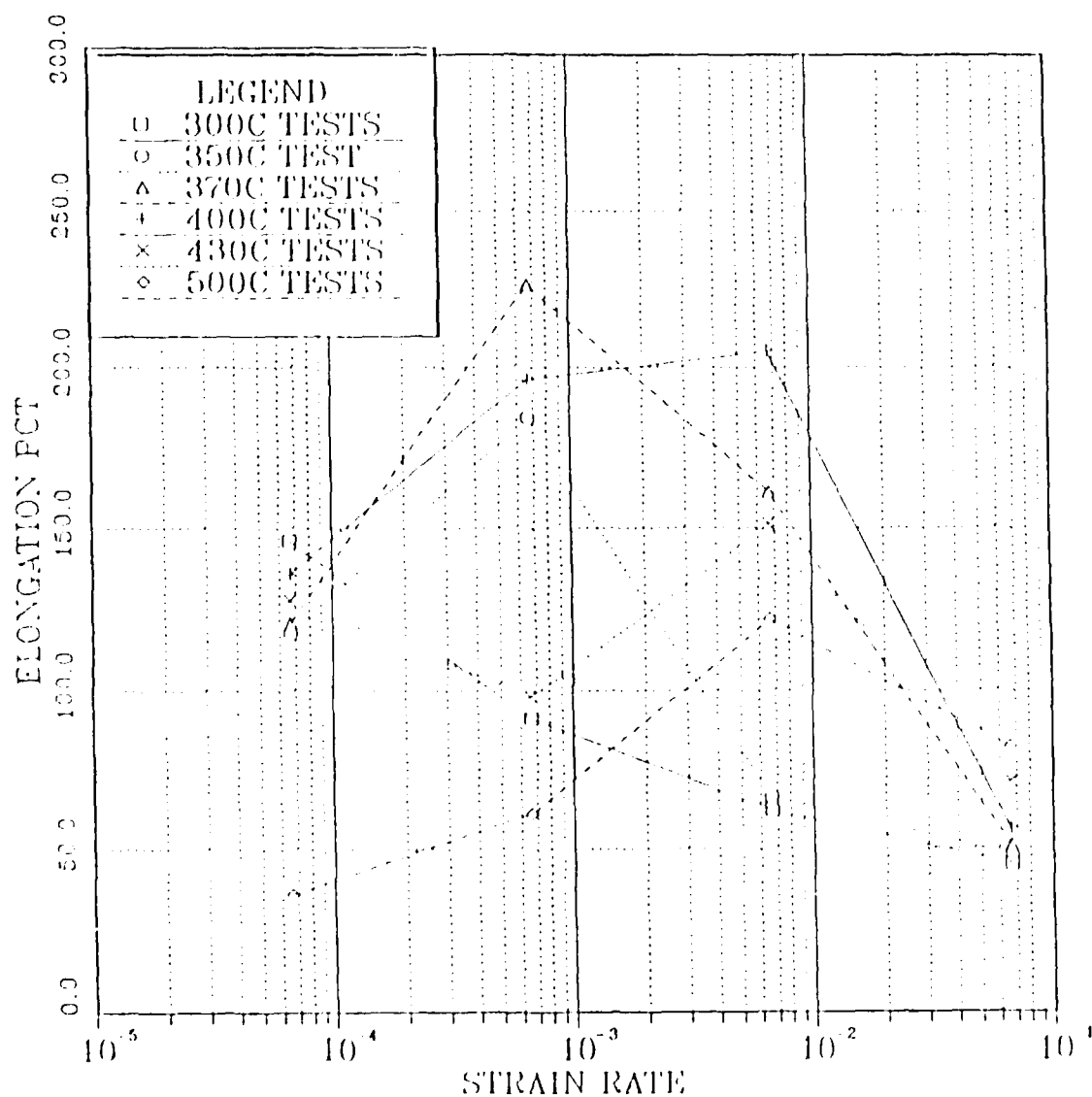


Figure B-4. Ductility vs. Strain Rate For Various TMP Schedules Shown In The Legend. The Material Was Rolled In The Original Plate Longitudinal Direction With True Strain Of 2.60 At Lower Rolling Speed.

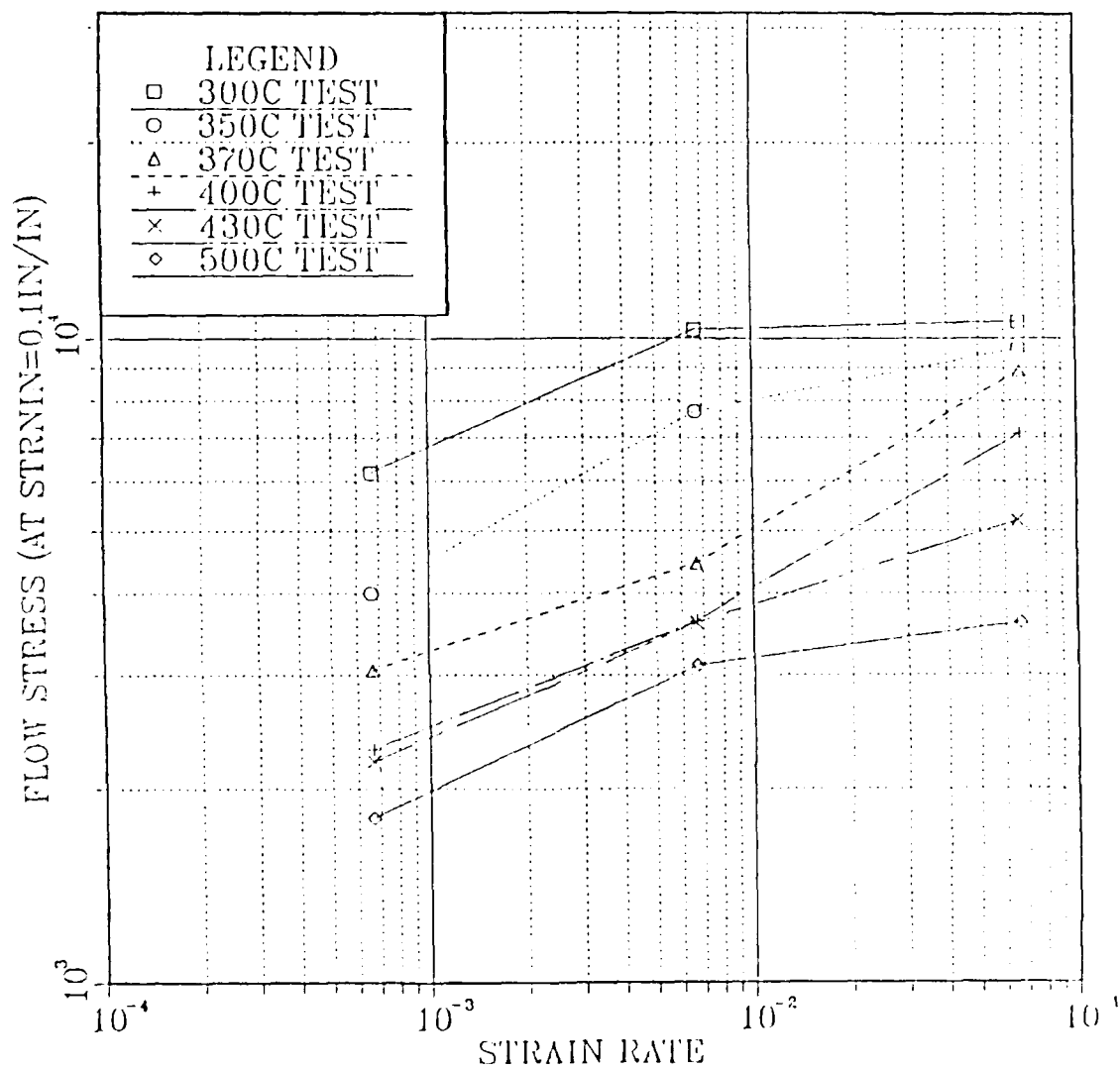


Figure B-5. Flow Stress vs Strain Rate At Strain Of 0.1  
For Material Rolled To 2.60 True Strain  
At Lower Rolling Speed.

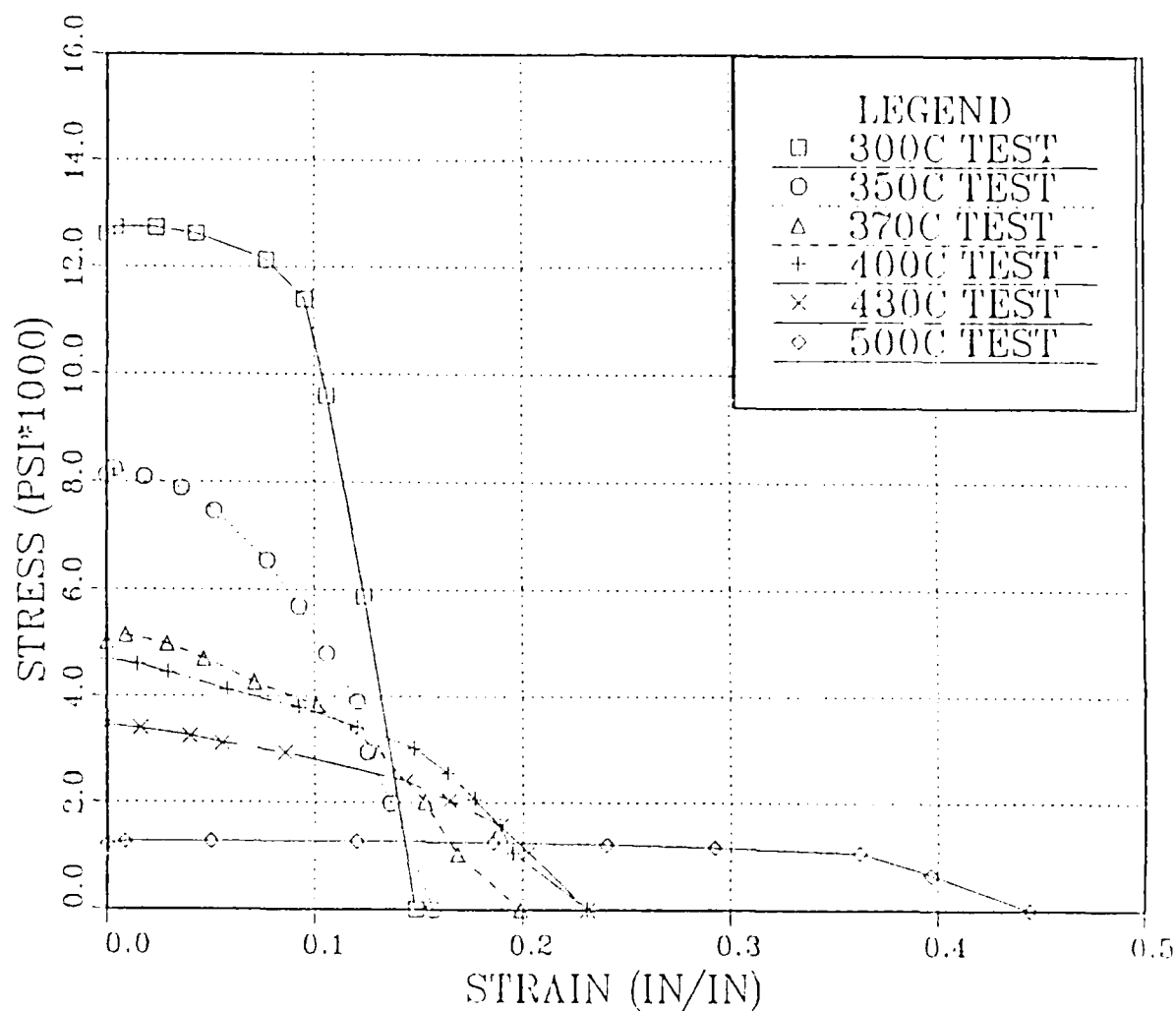


Figure B-6. True Stress vs. True Strain As Function Of Test Temperature At A strain Rate of  $6.67 \times 10^{-4} \text{ S}^{-1}$ . The Material Was Rolled To A Rolling Strain Of 3.36 At 300 °C With 30 Minutes Reheating Interval between The Rolling Passes, In The Direction Parallel To The Original Plate Longitudinal Direction. The Specimens Were Annealed At 540 °C For 10 Minutes Prior To Testing

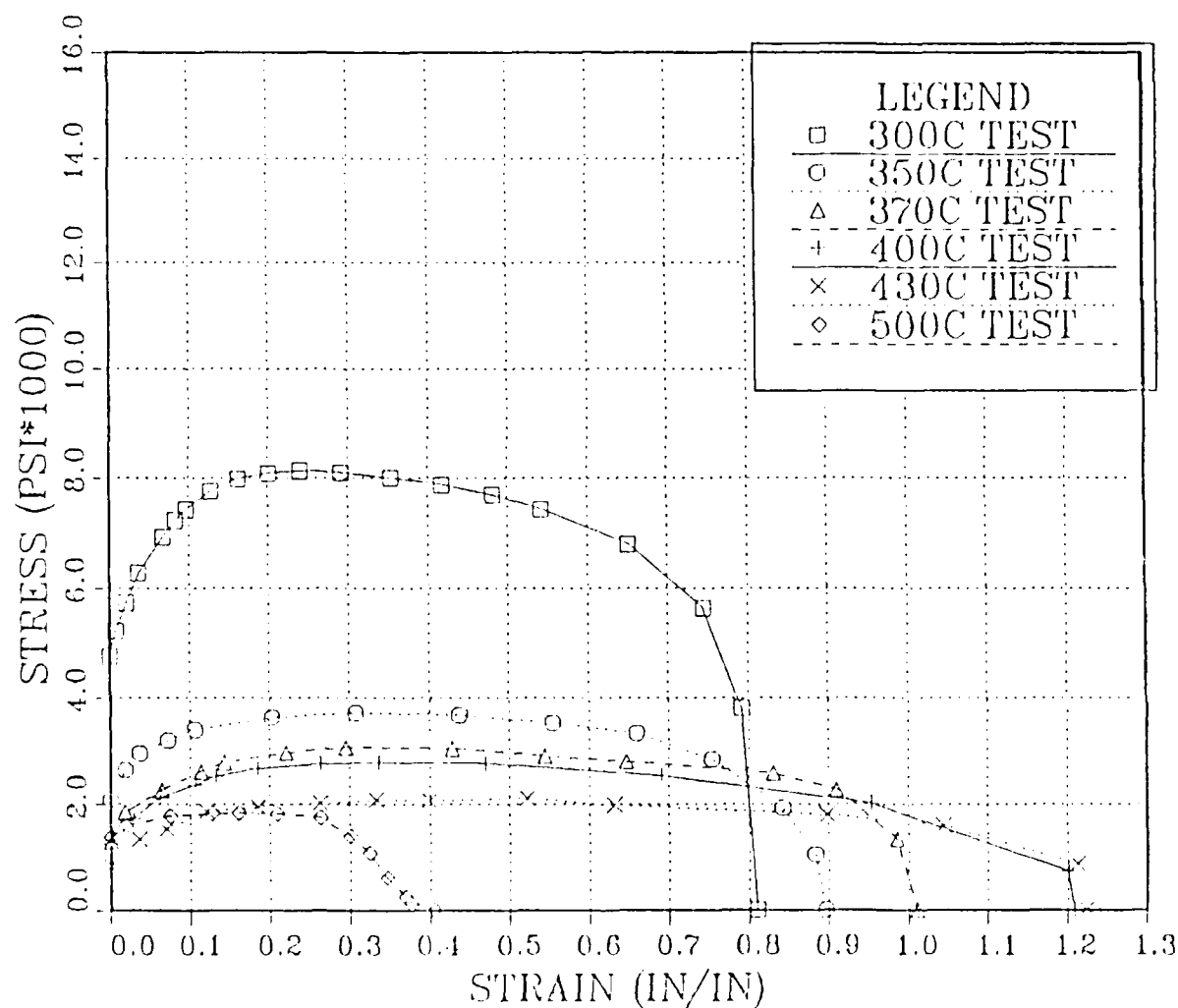


Figure B-7. True Stress vs. True Strain As Function Of Test Temperature At A strain Rate of  $6.67 \times 10^{-4} \text{ s}^{-1}$ . The Material Was Rolled To A Rolling Strain Of 3.36 At  $300^\circ\text{C}$  With 30 Minutes Reheating Interval between The Rolling Passes, In The Direction Parallel To The Original Plate Longitudinal Direction.



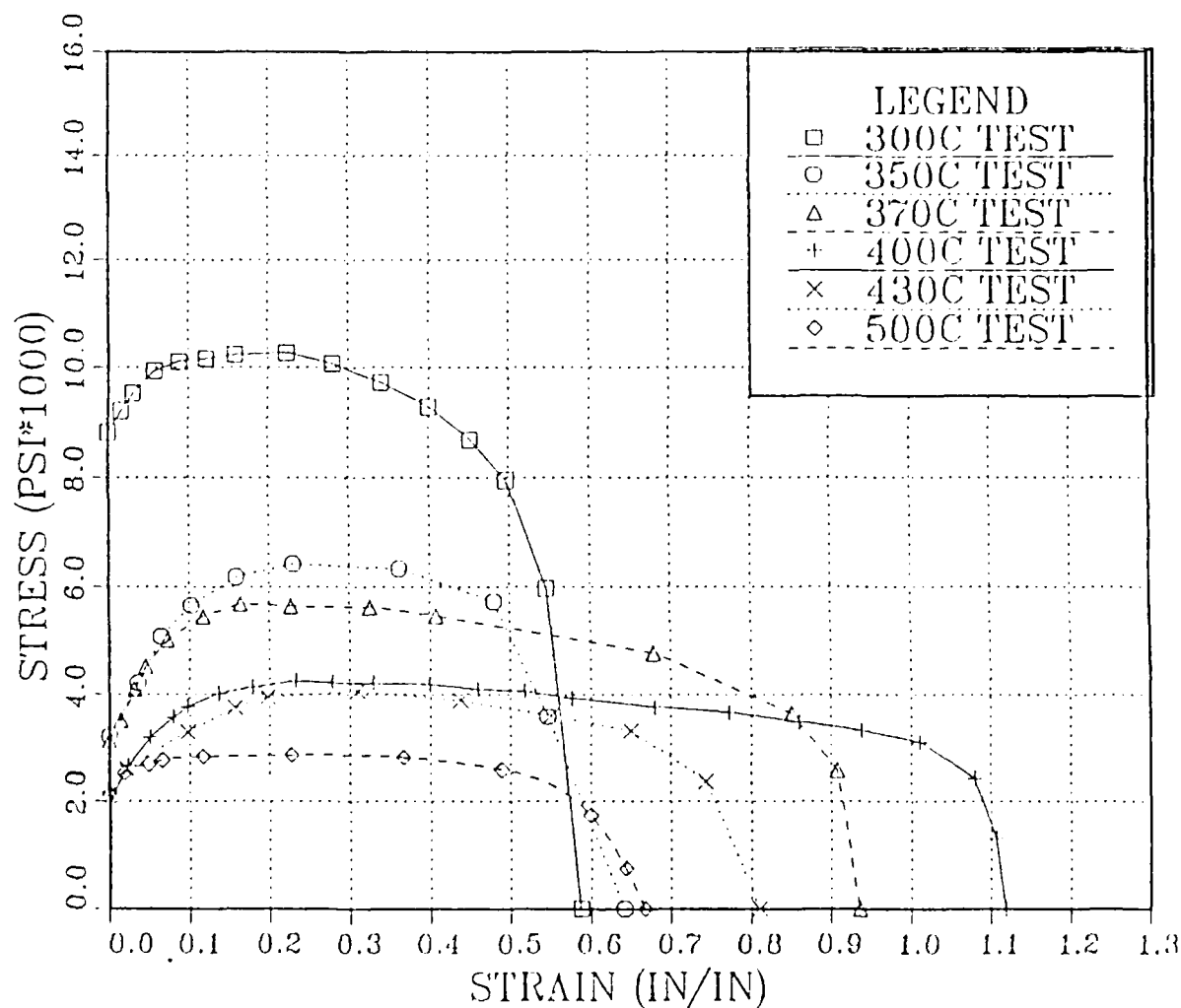


Figure B-8. True Stress vs. True Strain As Function Of Test Temperature At A strain Rate of  $6.67 \times 10^{-3} \text{ s}^{-1}$ . The Material Was Rolled To A Rolling Strain Of 3.36 At  $300^{\circ}\text{C}$  With 30 Minutes Reheating Interval between The Rolling Passes, In The Direction Parallel To The Original Plate Longitudinal Direction.

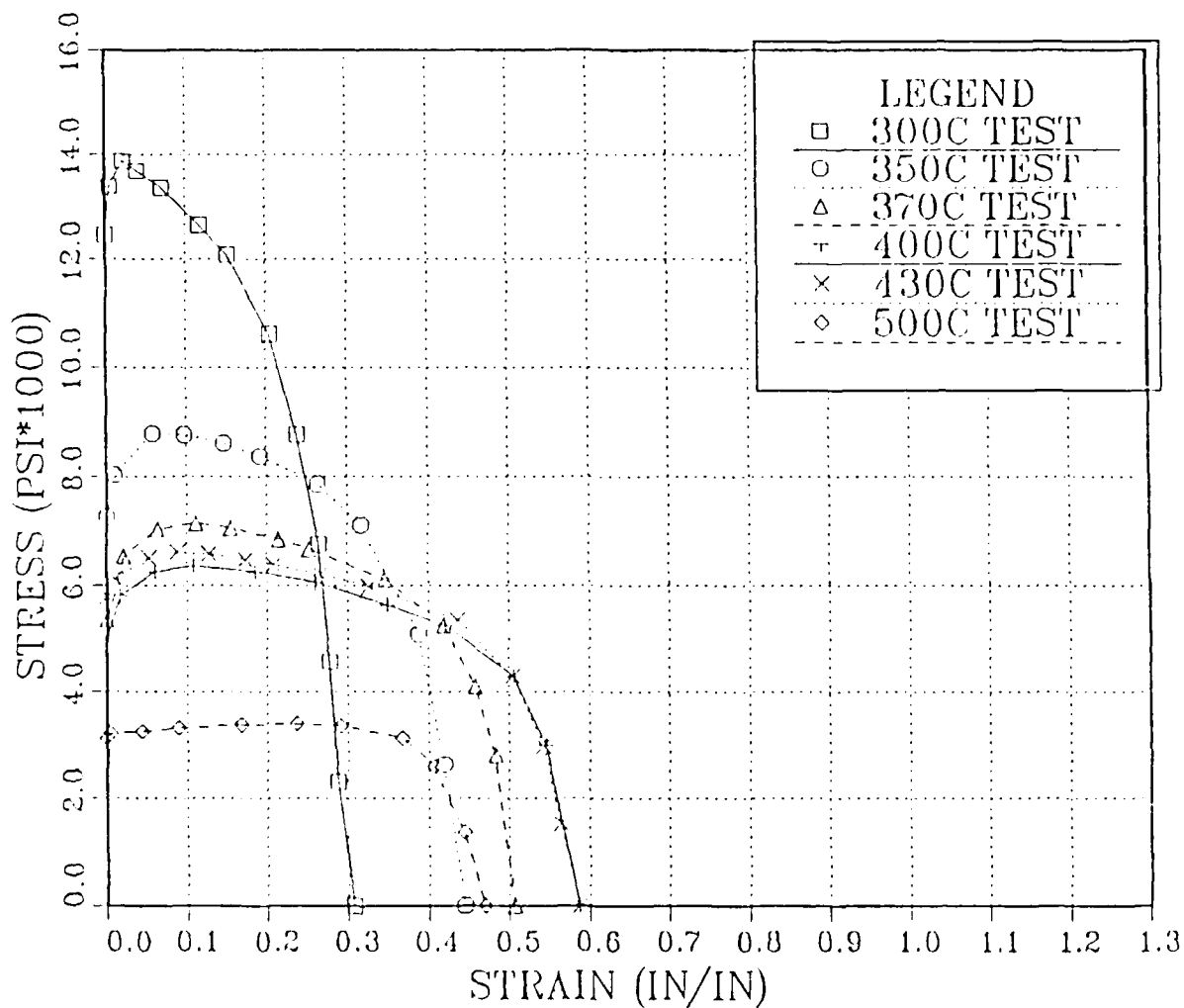


Figure B-9. True Stress vs. True Strain As Function Of Test Temperature At A strain Rate of  $6.67 \times 10^{-2} \text{ S}^{-1}$ . The Material Was Rolled To A Rolling Strain Of 3.36 At 300 °C With 30 Minutes Reheating Interval between The Rolling Passes, In The Direction Parallel To The Original Plate Longitudinal Direction.

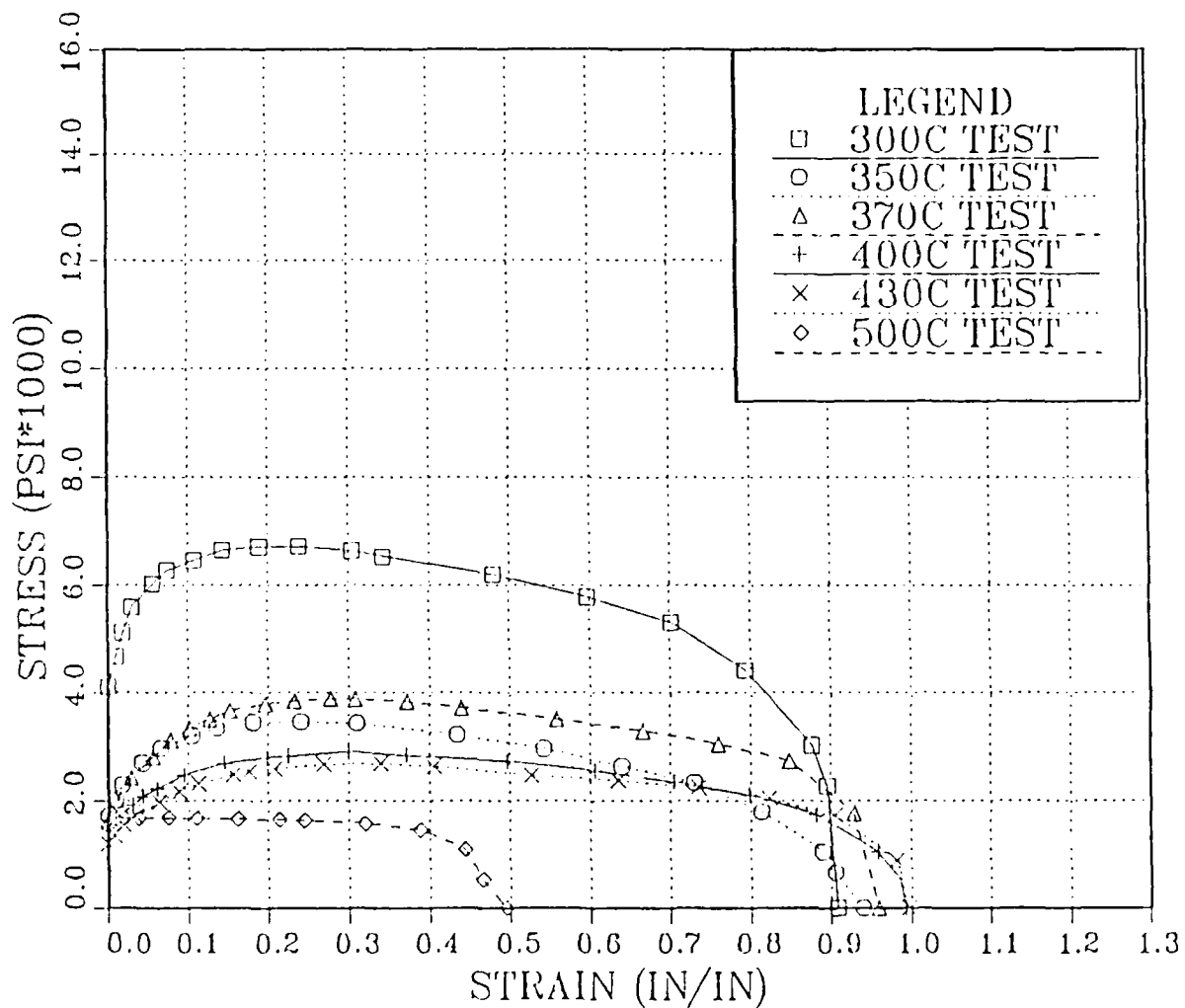


Figure B-10. True Stress vs. True Strain As Function of Test Temperature At A strain Rate of  $6.67 \times 10^{-4} \text{ s}^{-1}$ . The Material Was Rolled To A Rolling Strain Of 2.60 At 300°C With 30 Minutes Reheating Interval between The Rolling Passes, In The Direction Parallel To The Original Plate Longitudinal Direction At Higher Rolling Speed.

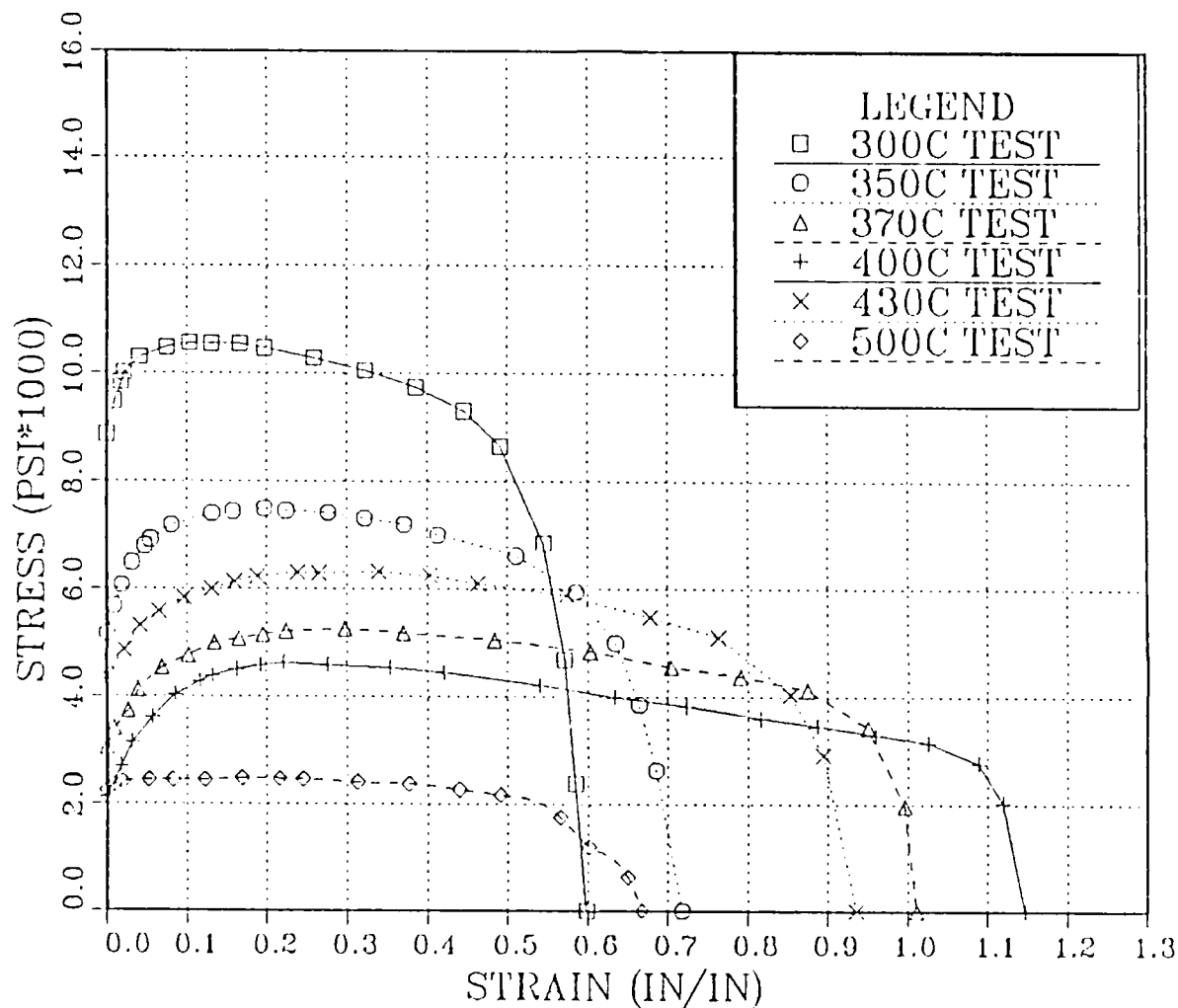


Figure B-11. True Stress vs. True Strain As Function Of Test Temperature At A strain Rate of  $6.67 \times 10^{-3} \text{ s}^{-1}$ . The Material Was Rolled To A Rolling Strain Of 2.60 At 300°C With 30 Minutes Reheating Interval between The Rolling Passes, In The Direction Parallel To The Original Plate Longitudinal Direction At Higher Rolling Speed.

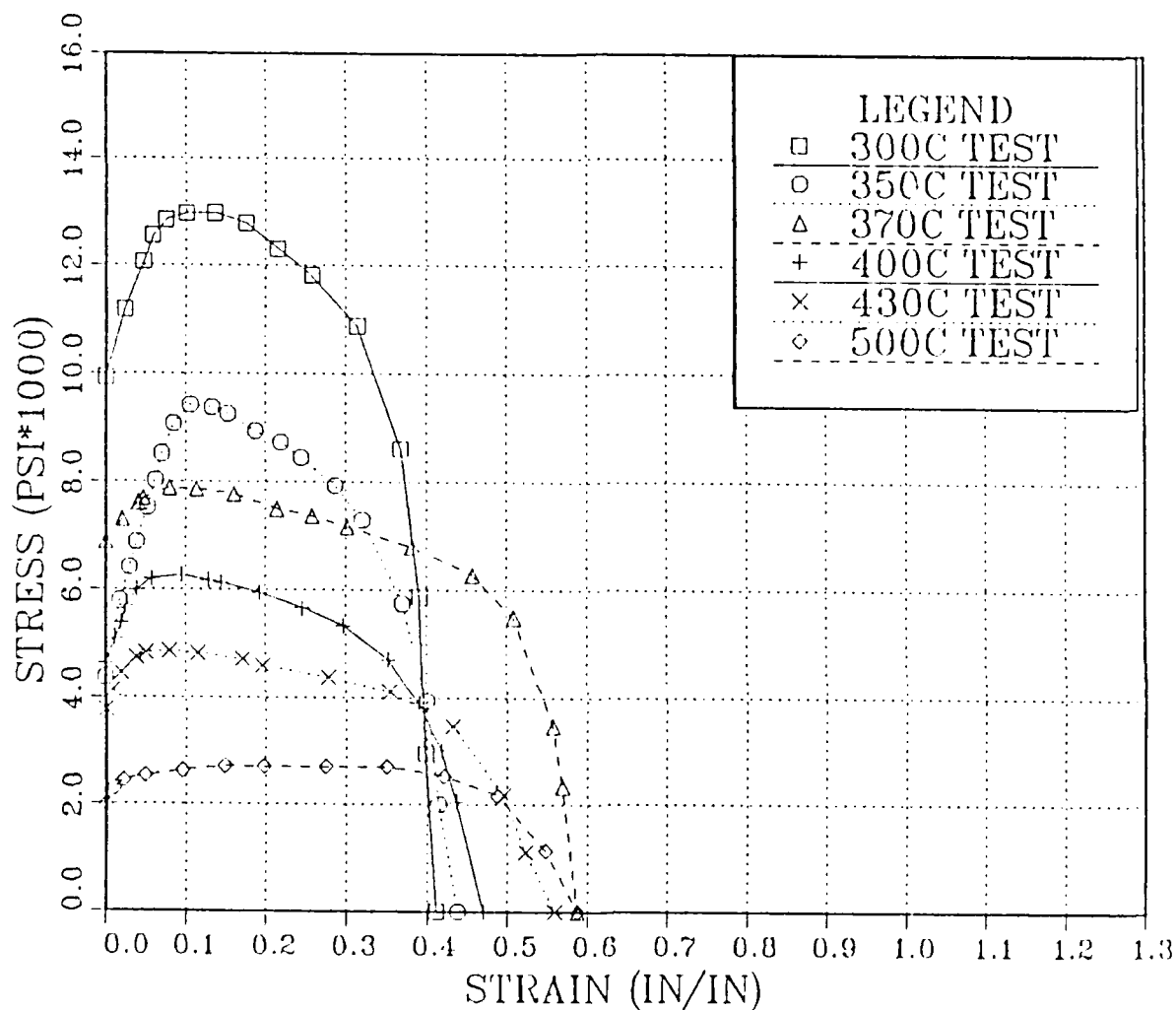


Figure B-12. True Stress vs. True Strain As Function Of Test Temperature At A strain Rate of  $6.67 \times 10^{-2} \text{ s}^{-1}$ . The Material Was Rolled To A Rolling Strain Of 2.60 At 300°C With 30 Minutes Reheating Interval between The Rolling Passes, In The Direction Parallel To The Original Plate Longitudinal Direction At Higher Rolling Speed.

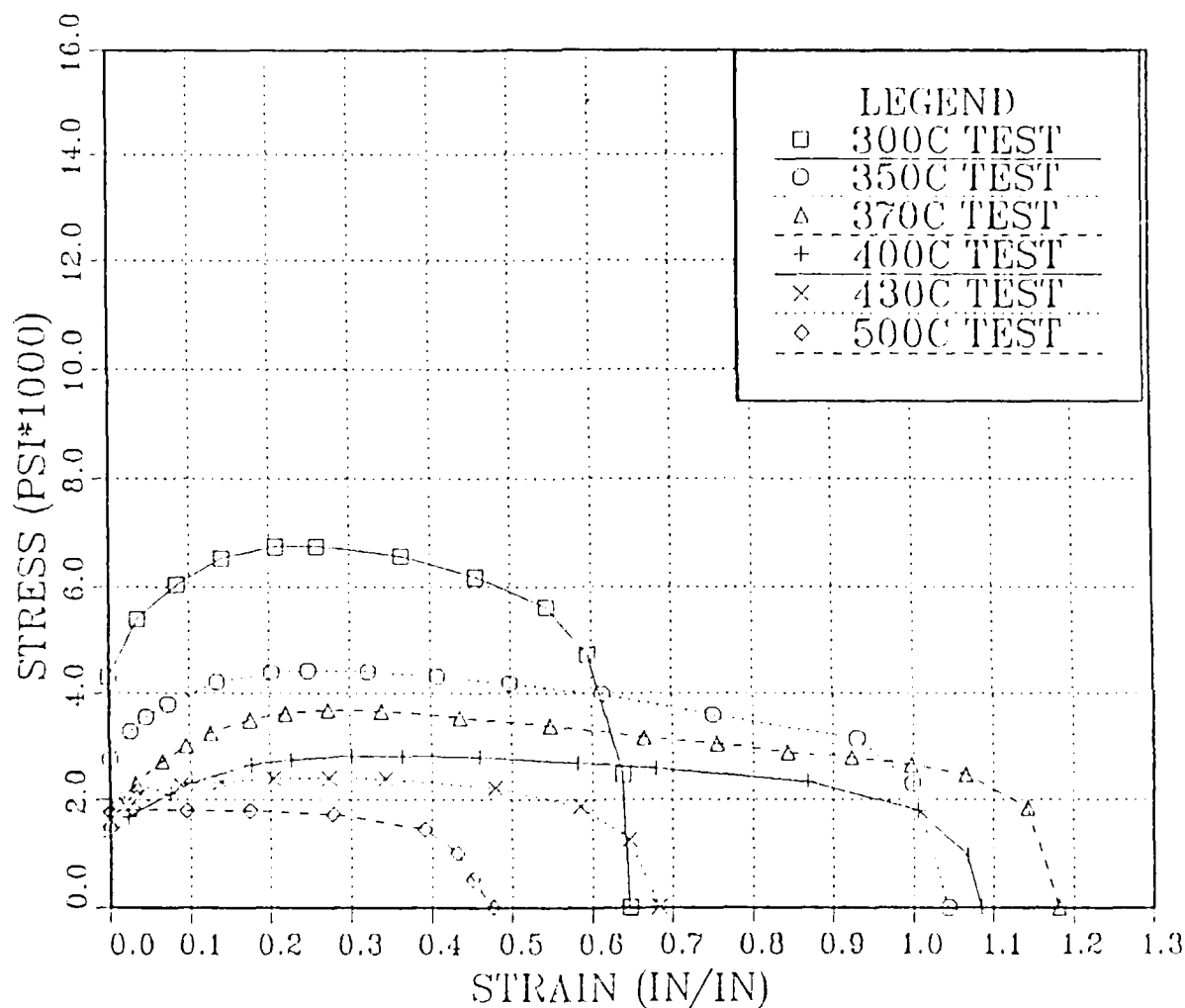


Figure B-13. True Stress vs. True Strain As Function Of Test Temperature At A strain Rate of  $6.67 \times 10^{-4} \text{ s}^{-1}$ . The Material Was Rolled To A Rolling Strain Of 2.60 At  $300^\circ\text{C}$  With 30 Minutes Reheating Interval between The Rolling Passes, In The Direction Parallel To The Original Plate Longitudinal Direction At Higher Rolling Speed.

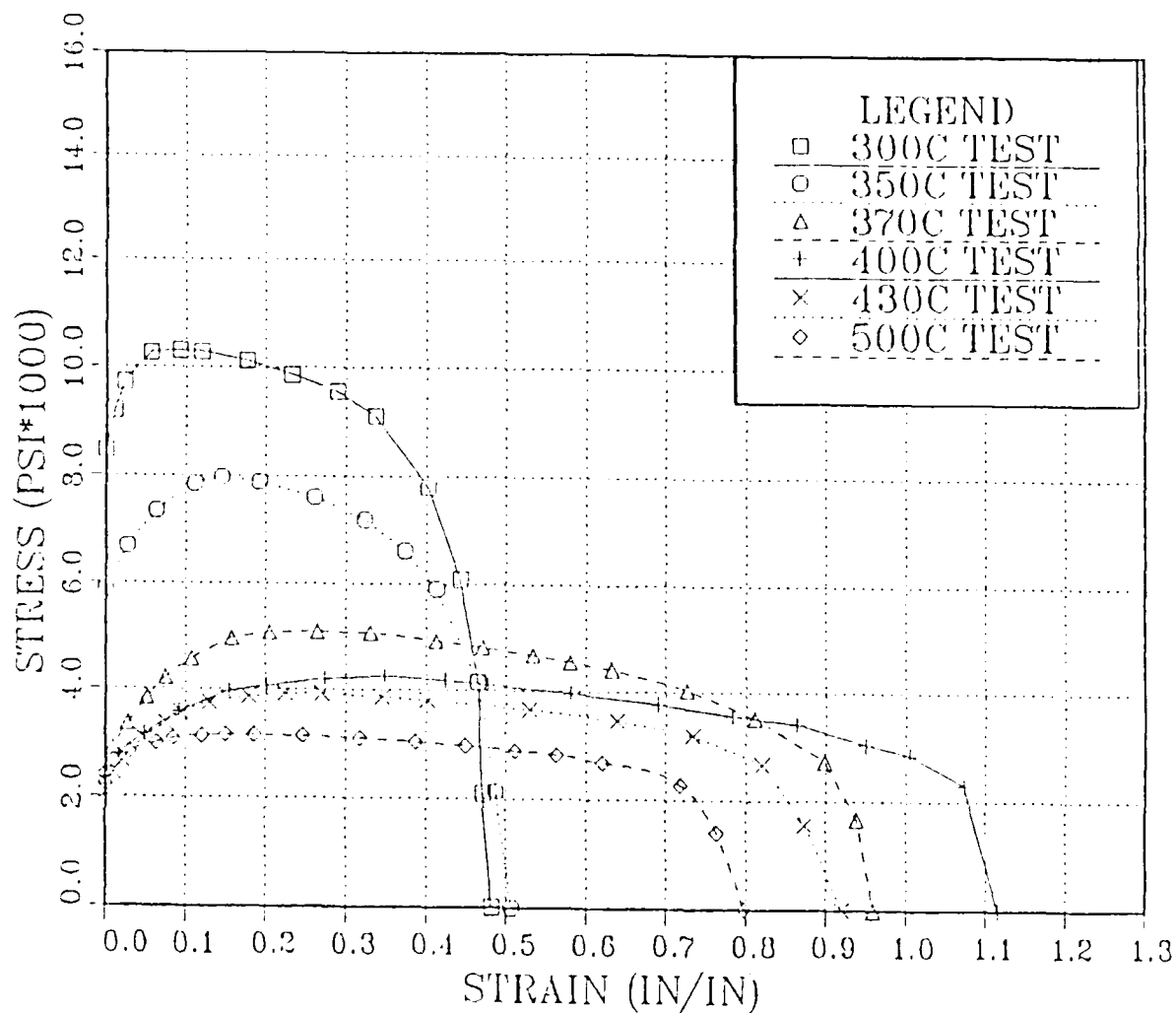


Figure B-14. True Stress vs. True Strain As Function Of Test Temperature At A strain Rate of  $6.67 \times 10^{-3} \text{ s}^{-1}$ . The Material Was Rolled To A Rolling Strain Of 2.60 At  $300^\circ \text{C}$  With 30 Minutes Reheating Interval between The Rolling Passes, In The Direction Parallel To The Original Plate Longitudinal Direction At Higher Rolling Speed.

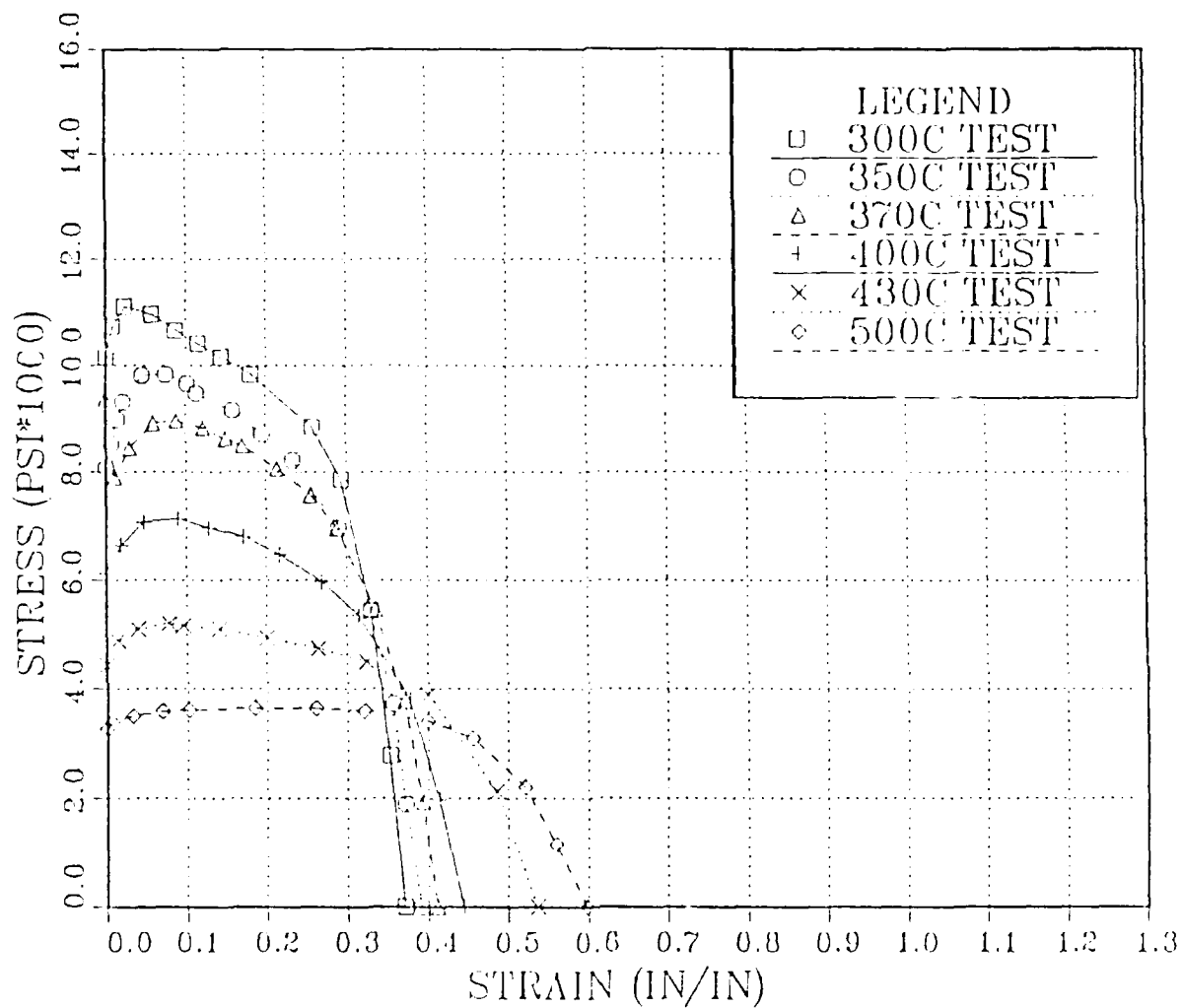


Figure B-15. True Stress vs. True Strain As Function Of Test Temperature At A strain Rate of  $6.67 \times 10^{-2} \text{ s}^{-1}$ . The Material Was Rolled To A Rolling Strain Of 2.60 At  $300^\circ\text{C}$  With 30 Minutes Reheating Interval between The Rolling Passes, In The Direction Parallel To The Original Plate Longitudinal Direction At Higher Rolling Speed.



## LIST OF REFERENCES

1. Michael B. Bever, Massachusetts Institute of Technology, Encyclopedia of Materials Science and Engineering V. 6, pp. 4783-4790, 1986.
2. Wadsworth, J., Nieh, T. G., and Mukherjee, A. K., "Superplastic Aluminum Alloys-A Review", Aluminum Alloys: Their Physical and Mechanical Properties, Volume II, edited by Starke, E. A. Jr., and Sanders, T. H. Jr., pp. 1239-1246, papers presented at the International Conference, held at the University of Virginia, Charlottesville, Virginia, June 1986.
3. Spiropoulos, P. T., Thermomechanical Processing of Al Alloy 2090 for Grain Refinement and Superplasticity, Master's Thesis, Naval Postgraduate School, Monterey, California, December 1987.
4. Askeland, D. R., The Science and Engineering of Material, pp. 324-326, PWS Publishers, 1984.
5. Lee, E. W. and McNelley, T. R. "Microstructure Evolution during Processing and Superplastic Flow in a High Magnesium Al-Mg-Alloy", Materials Science and Engineering, V. 93, pp. 45-56, 1987.
6. Regis, H. C. Processing of 2090 Aluminum Alloy for Superplasticity, Master's Thesis, Naval Postgraduate School, Monterey, California, June 1988.
7. Groh, G. E. Processing of Aluminum Alloy for Superplasticity, Master's Thesis, Naval Postgraduate School, Monterey, California September 1988.
8. Quist, W. E., Narayanan, G. H., and Wingert, A. L., "Aluminum-Lithium Alloys for Aircraft Structure - An Overview", Aluminum-Lithium Alloys II, edited by Sanders, T. H. Jr., and Starke, E. A. Jr., pp. 313-334, Conference Proceedings, TMS-AIME, Warrendale, Pennsylvania, 1984.

9. Bretz, P. E. and Sawtell, R. R, "Alithalite Alloys: Progress, Products and Properties", Aluminum-Lithium Alloys III, edited by Baker, C., and others, V. III, pp. 47-49, Conference Proceedings, Institute of Metals, London, 1985.
10. Bretz, P. E. "Alithalite Alloy Development and Production", 4th International Aluminum Lithium Conferences, edited by Champier, G, and others, pp. 25-31, Les Editions de Physique, Paris, 1987.
11. Underwood, E. E. "A Review of Superplasticity and Related Phenomena", Journal of Metals, pp. 914-919, December 1962.
12. Alden, T. H., "Review of Superplasticity", Treatise on Materials Science and Technology, V. 6.
13. Sherby, O. D., and Wadworth, J., "Development and Characterization of Fine-Grain Superplastic Materials", Deformation Processing and Structure, edited by Krauss, G., pp. 355-389, American Society for Metals, 1984.
14. Brandon, D. G., "The Structure of High Angle Boundaries", Acta Metallurgica, V. 14, pp. 1479-1484.
15. Hamilton, C. H., Bampton, C. C., and Paton, N. E., "Superplasticity in High Strength Aluminum Alloys", Superplastic Forming of Structural Alloys, edited by Paton, N. E., and Hamilton, C. H., pp. 173-189, Conference Proceedings, TMS-AIME, Warrendale, Pennsylvania, 1982.
16. Wert, J. A., "Grain Refinement and Grain Size Control. Superplastic Forming of Structural Alloys", edited by Paton, N. E. and Hamilton C. H., pp. 69-83, Conference Proceedings, TMS-AIME, Warrendale, Pennsylvania, 1982.
17. B. M. Watts, and other, "Superplasticity in Al-Cu-Zr Alloys Part II: Microstructural Study", Metal Science Journal, V. 6, pp. 189-198, June 1976.

18. Ricks, R. A. and Winkler, P. J., "Superplastic Optimization for Diffusion Bonding Applications in Al-Li Alloys", Superplasticity and Superplastic Forming, edited by Hamilton, C. H., and Paton, N. E., Conference Proceedings, TMS-AIME, Warrendale, Pennsylvania, 1988.
19. Hales S. J. McNelley T. R., "Fine-Grained Superplasticity at 300 °C in a Wrought Al-Mg Alloy" Superplasticity in Aerospace, edited by Heikenen, H. C., and McNelley, T. R., pp. 61-76, Conference Proceedings, TMS-AIME, Warrendale, Pennsylvania, 1988.
20. Hales S. J., McNelley T. R., and Groh G. E., "Intermediate Temperature Thermomechanical Processing of Al-2090 for Superplasticity", Aluminum Lithium Alloys V, edited by Sanders, T. H., and Starke, E. A., Conference Proceedings, EMAS, Wareley, U.K., in press, 1989.
21. Dieter G., Mechanical Metallurgy, pp. 297-300, McGraw-Hill Book Company, 1976.
22. Encyclopedia of Science and Technology, V. 8, p. 180, McGraw-Hill Book Company, 1987.
23. Crooks, R., Hales S. J., and McNelley, T. R. "Microstructural Refinement via Continuous Recrystallization in a Superplastic Aluminum Alloy", Proceedings of International Conference, on Superplasticity and Superplastic Forming, Blaine, Washington, August 1988.
24. George F. Vander Voort, Metallography, Principles and Practice, pp. 196-199 and 610, McGraw-Hill Book Company, 1984.
25. McQueen H. J., "The Experimental Roots of Thermomechanical Treatments for Aluminum Alloys", Thermomechanical Processing of Aluminum Alloys, edited by James G. Morris, p. 11, Conference Proceedings, the Metallurgical Society of AIME, October 18, 1978.

# INITIAL DISTRIBUTION LIST

	<u>No. Copies</u>
1. Defense Technical Information Center Cameron Station Alexandria, Virginia 22304-6145	2
2. Library, Code 0142 Naval Postgraduate School Monterey, California 93943-5002	2
3. Department Chairman, Code 69Hy Department of Mechanical Engineering Naval Postgraduate School Monterey, California 93943-5000	1
4. Professor T. R. McNelley, Code 69Mc Department of Mechanical Engineering Naval Postgraduate School Monterey, California 93943-5000	5
5. Naval Air Systems Command, Code AIR 931 Naval Air Systems Command Headquarters Washington, D. C. 20361	1
6. Dr. S. J. Hales NASA-Laugley Resident Ctr. Mail Stop 188A Hampton, Virginia 23665-5225	1
7. Dr. Eui-Whee Lee, Code 6063 Naval Air Development Center Warminster, Pennsylvania 18974	1
8. Deputy Chief of Naval Staff (M) Naval Headquarters Islamabad Pakistan	1
9. Assistant Chief of Naval Staff (Tech) Naval Headquarters Islamabad Pakistan	1
10. Director, Ship's Maintenance and Repairs Naval Headquarters Islamabad Pakistan	1

- |     |   |   |
|-----|---|---|
| 11. | Director, Naval Construction<br>Naval Headquarters<br>Islamabad<br>Pakistan   | 1 |
| 12. | Director, Naval Training<br>Naval Headquarters<br>Islamabad<br>Pakistan   | 1 |
| 13. | General Manager, PN Dockyard<br>Karachi<br>Pakistan   | 1 |
| 14. | Commanding Officer, PNS Jauher<br>Pakistan Naval Engineering College<br>Ch. Rehmatullah Road<br>Karachi-8<br>Pakistan | 1 |
| 15. | Commandant PAF Aeronautical<br>Engineering College<br>Resalpur<br>Pakistan  | 1 |
| 16. | LT CDR M. B. Choudhry<br>PNS Jauhar<br>Ch. Rehmatullah Road<br>Karachi-8<br>Pakistan                                  | 2 |